Version061225

EXPERIMENTAL AERODYNAMICS AND CONCEPTS GROUP

GEORGIA INSTITUTE OF TECHNOLOGY

School of Aerospace Engineering, Atlanta GA 30332-0150

Tailored Force Fields, Phase 2

Final Report, December 2006

Experimental Aerodynamics and Concepts Group
School of Aerospace Engineering
Georgia Institute of Technology
North Avenue & Luckie St.
Atlanta GA 30332-0150
Phone 404-894-9622 • Fax 404-894-2760

1 Introduction

This document captures the state of progress on Tailored Force Fields, at the end of a Phase 2 study sponsored by the NASA Institute of Advanced Concepts. The concept has progressed from reduced-gravity flight demonstrations through architecture studies, system concepts and first-principles based validation through a doctoral dissertation with NASA mentorship. In this report, the key issues are summarized, and a roadmap for future work is presented.

1.1 Why Tailored Force Fields?

The long-term potential of this project is that it explores a way to build the large, massive infrastructure in Space, needed for permanent human habitats and extraterrestrial resource exploitation. The key technology is one that enables automatic construction using solar energy and extraterrestrial material.

In the 1970s, several visionaries, Gerard O'Neill most prominent among them, argued that the best habitats for humans living away from earth to conduct space-based manufacturing, repair, supply and exploration, would be orbiting cities, rather than on or under planetary surfaces. In-depth studies were conducted by NASA/ASEE in the late 1970s. Humans (at least the present state of evolution) need a gravity level near that found on Earth's surface (1G) for long-term living. Habitats built along the inner circumference of a rotating wheel or cylinder can simulate gravity to a desired extent. However, a current thumbrule is that rotation rates must be below 1rpm to spare most people from disorientation. It is easily seen that a wheel with 1G at the rim at less than 1G, has a radius on the order of a kilometer. Building such a structure in space is a daunting undertaking.

Radiation shielding is the other show-stopper to plans for human exploration and development of space. Recent work by NASA suggests that roughly 0.5 m thickness of lunar regolith will suffice to effectively stop all forms of space radiation to the level needed to avoid limiting human tenure in space. A shield for a station large enough for long-term habitation is obviously too massive to contemplate launching from Earth. Human labor in assembling the shield is also ruled out. These problems have essentially killed off ambitions to build cities in space. The NASA/ASEE studies tried to minimize exposed surface area with tubular-rim stations, but still found it impossible to build the radiation shields for them, even at the ludicrously-optimistic STS launch cost projection of $100/lb to LEO.

1.2 Origin of the TFF concept

In 1997, an experiment by Georgia Tech undergraduates on NASA's Reduced Gravity Flight laboratory (a.k.a. "Vomit Comet") demonstrated an interesting phenomenon, that they called "Acoustic Shaping". Random-shaped particles placed inside a box, driven at one of its resonant frequencies with an acoustic speaker, would form into walls along the predicted nodal surfaces in low gravity. The implications of this finding led to the question of what happens in an electromagnetic resonator, and the size and power requirements to build large structures in deep space. In particular, the TFF technology offers a way to solve the problem of adequate long-term radiation shielding. Other implications are that the structures being conceived are large enough to enable 1-G, spacious, safe shirtsleeves environments and large-volume storage. With such infrastructure in orbit, the present stranglehold of earth-launch costs will be broken, and one can visualize a massive Space-based economy that will dwarf today's terrestrial economy.

1.3 Concept Development, Phase 1

In Phase 1, we first considered the problem of how to build large "Space cities". We showed an approach using lunar material and a systematic lunar-based development that would span a ten-year period of automatic construction, with telepresence supervision. The point made there was that a comprehensive plan for a space-based economy (as opposed to fragmented plans for specific projects) would enable even a plan as ambitious building a 2km-diameter, 2-km long cylinder, radiation-shielded to 2m depth, at a reasonable cost to the taxpayer. The key was to cross- link concepts so that the expensive supplies for one

concept were the by-products of another concept, and where each entrepreneurial concept had a guaranteed market for a sufficient period to cut down their market risk.

This demonstration thus removed the notion that large projects had to be outrageously expensive in taxpayer dollars.

In addition to the prerequisite infrastructure and economic basis for launching mass from the Moon, the above approach to building stations required telepresence and a large number of individual construction operations for the basic structure. We then turned attention to the more interesting technical problem of how massive structures might be built automatically in deep space, using force field tailoring. Acoustic construction could not be scaled up to the size needed to form a habitat module in one operation, and hence we investigated electromagnetic analogues of the concept, which could work in a vacuum.

Our first breakthrough was the finding of experimental evidence and theory that indicated the commonality between the phenomena behind results from optical manipulation of nano-materials and our observations in acoustics. Similarities were found in the mechanisms of the primary force field that accelerates particles towards desired locations, between electromagnetic and acoustic fields, in the regime where particle size is much smaller than wavelength (Rayleigh regime). This finding was used to develop a rudimentary scaling relationship involving particle size, wavelength and material properties, for the acceleration per unit intensity experience by a particle in an electromagnetic or acoustic field. Away from Earth but at Earth's orbit around the sun, we showed that an acceleration level of 1 micro-G was adequate to dominate over any other accelerations due to other forces.

We selected a 50m diameter, 50m high cylindrical module, shielded to 2m depth, as a test case, and showed that the input power needed to a radio-wave resonator in order to form such a module from a cloud of 20cm-diameter rocks, could be provided by a 2 square-kilometer, 10% efficient solar cell array. The power needed was much lower than that used by the Arrecibo radio telescope in the 1970s to beam a 3-minute signal into space as part of the SETI program. The values obtained are shown in Table 1.1

Example: Construction of a 50m dia cylinder at Earth-Sun L-4 from NEO material radiation-shielded, 1-G Station at Earth-Sun L-4:
Particle diameter: 0.2m Wavelength: 100m Particle acceleration: 10-6 g Resonator intensity: 328 MW/m2 Resonator Q-factor: 10,000 Beam diameter = 100m
Power input: 258 MW Active field time: 13 hrs Solar Collector efficiency: 10% **Collector area w/o storage: 2 . sq.km**

Table 1-1: Order of magnitude estimates to size the solar power requirements for building a large radiation shielded module using

In Phase 2, we focused on detailing the architecture to construct large structures using the TFF technique, and on validating the technology through a large range of particles sizes and wavelengths.

In this document, we summarize the work already presented through several publications on the various issues. The report is organized as follows. The first section summarizes the architectures considered, for exploiting and advancing the Tailored Force Fields concept. Next, the progress towards validating the technology and developing a prediction and simulation capability, is summarized. Following this, discussion is focused on the systems to perform the "extreme" mission of extracting construction material from a Near Earth Object . The roadmap for future work is laid out, followed by lists of degrees awarded, publications and public interest/ outreach.

1.4 Summary of Feasibility

There are no show-stoppers identified so far, towards building large structures using extraterrestrial material from NEOs using force-field tailoring. Of course there is much development remaining to be done. Two major findings redirected the emphasis from the one-shot mission to build massive habitats as single pieces, towards an approach where mass from deep Space will be brought to earth orbit, and the structures built within telepresence reach.

The first finding is that the mechanisms of secondary force generation, involving particle-particle and particle-field interactions, are critical in determining what structures are formed. This shows that electromagnetic fields can be used to build thin solid elements such as bars, rings and other structural members, while acoustic fields are probably best suited to forming entire walls on a much smaller scale. This finding favors construction techniques where structural elements are first formed, with loose material being used to fill walls as needed for radiation shielding.

The second finding is that powerful lasers suitable for cutting rock, can be powered directly by broadband solar energy. This finding opens the way to a large mass savings in the conversion equipment currently needed to go from broadband solar energy to laser power supplies. With this route open, missions using solar sails/collectors can be developed, to visit near-Earth Objects, collect mass, and return to Earth orbit.

Combining the above two approaches, the architecture to build large, massive stations using force field tailoring is made much more feasible in the medium term, without waiting for any large-scale economic development of extraterrestrial resources or a Space economy.

The technology of force field tailoring has been interlinked and validated through four orders of magnitude, a size range where several different phenomena are encountered. Actually building large structures requires validation of the technology through another 3 to 4 orders of magnitude, but in this range, no fundamental changes in phenomena are anticipated. The roadmap for further development sees two steps as critical. The first is a simulation capability that permits detailed design or structures formed using tailored force fields. The second is a demonstration experiment at the 100mm diameter scale of solid objects, of the primary and secondary forces acting on particles in a long-wave electromagnetic field.

2 Architecture

2.1 The Context For Building Massive Structures In Orbit

Large space stations will not be built for science alone – the budget and incentives must come from beyond just a national space program. There are 3 reasons to build a massive structure in orbit rather than on a planetary surface:

- It is a habitat for humans who must commute to workplaces in orbit, e.g., power satellites, manufacturing facilities or for maintenance functions.
- It is a long-duration mission, such as a mission to Mars. Further, it is likely to be a routine mission, such as a Cycler[1] that stays in orbit, or perhaps a military earth-observation station that requires human presence.
- It is a tourist hotel with some staff stationed for long durations.

Any of these presupposes planning towards a space economy, with one or more of the following present:

- Space-based large-scale manufacturing or solar power plants.
- Regular missions to Mars or other planets (again presupposes an economy there)
- Routine launches from earth inexpensive enough to support a flourishing tourist business.

This does not presuppose that low-cost services exist already – just that such interests are involved in the planning.

In this discussion, we consider space stations intended as outposts for the first human explorers on long-duration missions in the solar system, presumably for resource development. This is conceived as occurring in a near-term space economy development plan, tied where possible into the present NASA plans for exploration of the Moon and Mars. General choices are listed in Table 1.

Table 2.1: Morphological Matrix

Location of Construction/ Methods	Earth-Sun L4/L5	Earth Orbit	Earth-Moon L2/L5	Mars/Asteroids
Human Intervention	Robotic / delayed telepresence	Human presence	Telepresence	
Construction	TFF	Building Blocks	Space Debris Refit	Inflatables
Source of Material	Terrestrial	Lunar	NEO	
Construction Type	All at Once	Assemble Parts Made in Space	Assemble Earth-launched parts	Assemble lunar-launched parts
Radiation Protection	Physical Blocking	Electromagnetic Shielding	Water-filled walls	Hydrogen-filled walls
Adhesion Method	Sintering	Mechanical	Welding	Tensile elements
Power System	Photovoltaic	Nuclear	Fuel Cell	Solar direct conversion
Propulsion System	Chemical Rocket	Nuclear Rocket	Electric Propulsion	Solar Sails
			Total Possibilities	147,476

2.2

2.3 Broad Objectives & Constraints

The objective of the program is to solve the problem of building habitats in orbit, massive enough to provide radiation shielding and 1-G. The fixed criteria are given in Table 2. The requirement for complete radiation shielding is not excessive, since the craft/ structure should be designed for orbits that include segments of closer approach to the Sun. The requirement for 1G artificial gravity is somewhat arbitrary, since humans may adapt quite well to lower levels. However, there is insufficient data on the level needed for long-term human adaptation, and a 1G specification would permit lower

levels at different parts of the station, while ensuring that the station is designed to the strength needed for 1G. Note that the G specification is the primary criterion for structural strength.

Shield construction: Decider for extraterrestrial materials.
Radiation shielding must protect against high-speed massive particles (cosmic rays) as well as high-energy gamma rays and X-rays, and charged particles from the Sun, without generating lethal secondary emission that occurs when high-energy particles encounter metal skins. Per the rule of thumb cited above, a 0.5m is thickness of earth or lunar regolith (composed mostly of silicon dioxide) is adequate as a passive barrier to all types of radiation. It is easy to see that the radiation shield mass for a long-duration habitat must come mostly from extraterrestrial, low-gravity sources, if reusable machines can extract the mass.

Table 2.2 List of Requirements.		
#1	Launch Date	Deployment aimed at 2025
#2	Capacity of structure	Nominally intended to hold at least 50 people for long-term habitation, plus supplies, laboratories, greenhouse, micro-g access, and some resource extraction facilities
#3	Radiation Shielding	Complete radiation shielding in all working and living enclosures, so that level inside is no more than that indoors on Earth, when the structure is at 1 A.U. from the Sun.
#4	Artificial Gravity	1G at its living quarters (other parts of the structure may be at low or zero-G)
#5	Rotation Rate	Below 1 RPM threshold of disorientation, to accommodate 97% of population.

2.4 Quantitative Estimate of Mission Needs and Requirements

Table 2.3: Mission Needs and Requirements		
Need	**Rationale**	**Driving Requirement**
Compatibility with NASA ESAS for earth-launch	Use of CaLV, CEV and limited lunar resources/ development	#1
Volume needed	50m dia x 50m long cylinder modules (5)	#2
Mass for 5 modules	6,000 tons (0.5-foot thick at 2000kg/m^3)	#3
Strength	1G steady load due to rotation	#4
Mass of Support Structure	20 tons, primarily tensile elements.	**#4**
Station Radius	1000 m	#5

Why 50m cylinders? There is little precedent for choosing the size of a standard station module for long-duration human habitation in space. Since existing concepts for Mars Cyclers and Astronaut Hotels assume that all components are launched from Earth, they are necessarily derived from the dimensions of rocket parts, which in turn are limited by frontal area in order to reduce aerodynamic drag during ascent through the atmosphere. A long-duration, sheltered facility is likely to serve many functions including housing, laboratory space, vehicle docking and repair, medical / quarantine facilities, airlocks for extravehicular activity, food storage, preparation and even agriculture, common spaces, and playgrounds. Metaphors for such a self-contained, long-voyage station might include cruise ships, aircraft-carriers, or crude oil tankers, but with substantially more space per person. The 50m cylinder, 50 m high, was chosen to be compatible with a 100m wavelength in the initial concept analysis, and considered to pose an upper limit to the challenges that might be demanded of a new construction technique.

2.5 Links to the Present

The architecture specification for the present Moon-Mars Initiative defines NASA plans for launcher systems and extraterrestrial operations. Specifically, the Cargo Launch Vehicle is rated at 125,000 kg payload to LEO, with an estimated launch cost to LEO[2] of $8000/kg at the production rate envisaged for the present NASA plans. Table 4 lists several issues relevant to lunar operations and materials scenarios, along with an estimate of their present Technology Readiness Level[Error! Bookmark not defined.], and some rough guess of their probability of fruition. Table 2.5 lists several technologies being developed on Earth, and projects their level in the timeframe required for the habitat construction

project. Based on Tables 2.3 and 2.4, lunar resources are not used in the DMS baseline, since there is no reasonable probability of a high-capacity launcher operating routinely from the lunar surface before 2025. NEOs appear to be a better prospect at least as a low-gravity source of large mass for use in sending regolith into orbit.

Table 2.4: Lunar operations and materials scenarios

		TRL (est)	Year deploy	Readiness Probability
Power	SNAP-10A,500w, ZrH, U-235 Reactor, orbited 1957[3] Lunar-made solar cells[4]	8 6	2015 2020	0.5 0.3
Oxygen	ISRU	5	2020	0.5
Regolith	ISRU	5	2020	0.5
Metals	ISRU	5	2025	0.3
Other gases	ISRU	4	2025	0.2
Telepresence Operations	Earth-satellite – surface probe[5]	9	2015	0.9
Robotic Operations	Earth-satellite – surface probe[6], [7]	9	2020	0.9
Lunar commercial-scale launcher	Mass-driver	5	2025	0.5
NEO identification	Telescopes; flyby	10	2015	0.9
NEO rendezvous	Hayabusa followup	9	2020	0.9
NEO resources	Flyby; probes	4	2025	0.5

2.6 Alternative Mission Concepts & Architectures

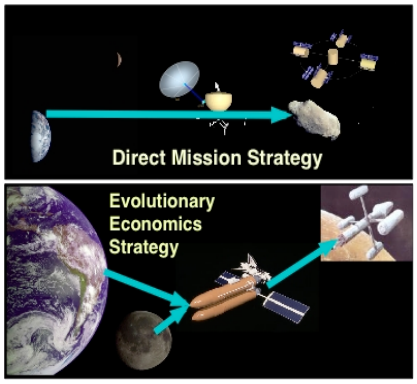

Figure 2-1:DMA vs. EEA: In DMA, the material is extracted and formed near a low-g object. In EEA, material from earth or other sources is formed into the structural skeleton, and filled with the shielding material

As seen in following chapters, work on Electromagnetic Shaping indicates that continuous chains of particles can be formed, providing control at a lower level (one more degree of freedom) than is possible using acoustics, where only walls can be formed. This makes intuitive sense, since electromagnetics involves vector fields as opposed to scalars. This raises a fundamental choice between two strategies:

The Direct Mission Strategy (DMS) is to build versatile construction machines and send them to low-gravity quarries of extraterrestrial material, to build a large radiation-shielded habitat. Presumably, such quarries will be Near Earth Objects, which can be reached with modest velocity increments.

The Evolutionary Economy Strategy (EES) is to manufacture small elements, integrates them with new markets in a Space economy, and then assembles parts into large structures. Presumably, in the latter case the mass will come from the Moon, and the construction will occur in the Earth-Moon system. This discussion starts evaluating the choices.

2.7 Direct Mission Architecture: Construction System Evolution

In the DMA (see Figure 2.1), the strategy is to send up a re-usable set of construction machines that can extract NEO material and build the external radiation shielded shells of several habitats with a standard module design. The size of the module is selected to pose a limiting case, rather than an optimized one. The construction is assumed to occur at a location such as earth-Sun L-4, which is at the same distance from the Sun as Earth, and is out of telepresence reach from Earth. For

conceptual design, a suitable NEO is assumed to exist at the construction location. In a later iteration, this design was tested on a construction mission to a specific NEO.

The architecture depends on two robotic systems. The first is a multipurpose craft called the "Rockbreaker" (Figure 2.2). This craft is to rendezvous with a suitable NEO, selected for its negligible spin, and rocky material.

After attaching itself to the NEO, the device is to use its cutting arms to generate the proper size particles (construction blocks) for the TFF generators. Vanmali et al[8] described an Integrated Rendezvous Anchoring Maneuvering System (IRAMS) to attach the Rockbreaker to a microgravity NEO. This system is a combination of 4 pulsed solid-grained plasma thrusters that double as manevering units and impact torque screwdrivers. At the final moment of touchdown, the thruster reverses, and the reaction to its impulse is transmitted through the solid grain into a torque to drive a deep-thread augur into the surface. Once attached to the surface, the two telescoping cutting arms deploy, and the 60 hybrid plasmajet-sheathed laser cutters dig trenches in spiral patterns on the ground around the lander. Each cutter is a truncated linear aerospike nozzle, where the plasma jet forms the outer sheath, and the laser beam comes out of the truncated base. The cutting laser beam is protected in a plasmajet sheath which serves to clear away the melt from the laser beam, and provide the pressure inside the trench that lifts blocks of required size out of the trench, and sends them floating into space at the desired velocity, overcoming the weak gravity field of the NEO. Thus the cutting action of the two arms generates a helical cloud of blocks of the NEO material, floating slowly away from the NEO.

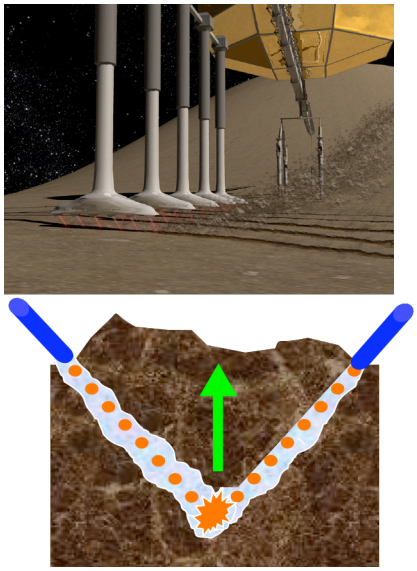

Figure 2-2:Rockbreaker: Conceptual Sketches. Above, Laser/plasmajet nozzle manifolds cut trenches in a helical pattern. Below, detail of trench-cutting showing laser pulses fracturing the soil, and plasmajet pressure lifting the material out of the trench

2.8 A. TFF System Operation Overview

The arrangement to form a cylinder from the rubble floated up by the Rockbreaker, is shown in Figure 2.3. The TFF system consists of four robotic spacecraft, which arrange themselves into a Fabry-Perot resonator. The intense radio-frequency field inside the resonator forms the rubble into a cylindrical shape. Higher-frequency beams from arms attached to the resonator (or to the Rockbreaker if possible) are used to sinter the rubble in place, providing enough strength to hold the cylinder together in zero-gravity when the field is turned off. Subsequent layers of rubble are formed concentrically on the first cylinder using slightly different modes of excitation, and sintered in place.

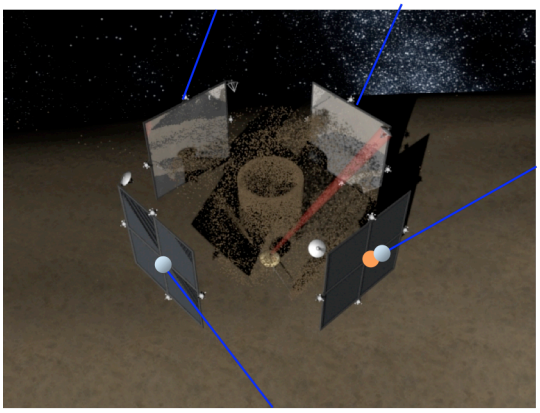

Figure 2-3:The four sides of the TFF resonator, shown moving away after forming a cylinder. The Rockbreaker is shown far below on the NEO surface, with power beamed to it. The long rods extend to the solar sail/collectors which are not shown.

2.8.1 Formation and Sintering Operation

The sintering operation commences as one of the

side walls of the resonator moves away allowing a second Rockbreaker craft to access the side and beam energy onto the particles, with the resonator spinning slowly about its axis relative to the particles held in the cylindrical wall inside.

Depending on the desired thickness and construction of the habitat walls, multiple walls may have to be formed. There are different options for this. One option is to form another layer of rocks around the first, using a slightly different mode. Another is to form several interspersed rings. In the EM field, switching to another mode can induce attraction between the wall and new incoming particles, forming thicker walls. These would have to be sintered in place. The sintering is a laborious process requiring considerable robotic intelligence, maneuvering of the sintering arm, and perhaps the whole craft, and hence will consume propellant, but the pace required is slow. Vanmali et al[8] calculated that this process would take roughly 19 hours (not 19 days as written in that paper) to form and sinter 10 layers of 20cm thickness each. The limiter on rate is the cutting rate. During this time, the resonator would have to move at near-constant speed relative to the NEO to stay with the spiral cloud of blocks being sent up. With the 0.5m shell thickness now sought, the time would come down by a factor of 4 or more.

2.8.2 Finishing assembly

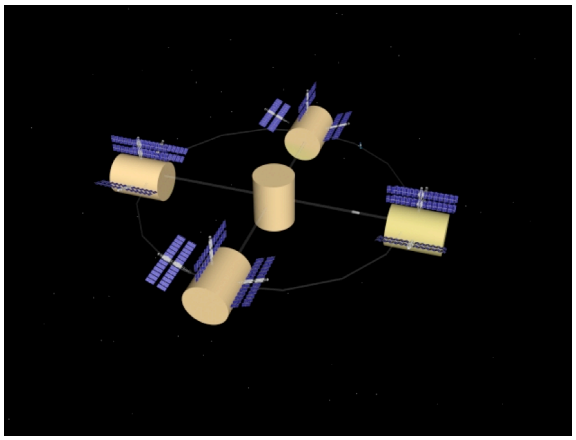

Figure 2-4: : 1-G Station comprised of five 50m radiation-shielded cylinders

The rest of the construction of the station and the assembly of the five modules, can be accomplished using smaller robotic craft, with the help of the RockBreakers. Figure 2.5 shows a completed 5-module station.

2.8.3 Refueling the Rockbreakers

Figure 2-5: Artist's conception of the TFF system, with a 1km x 1km solar array

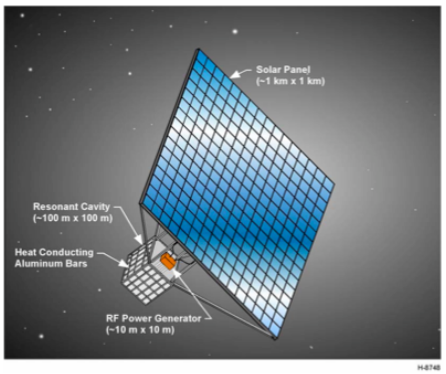

Artist's rendering of space craft system assembled in orbit.

The maneuvering propellant and cutting gas of the Rockbreakers can be common, and hence a refueling operation can be done with a single rendezvous with a tanker sent from Earth. Refurbishment of the lasers and the NEO-rendezvous IRAMS thrusters poses a tougher challenge, but again may be accomplished by ejecting old thrusters, one leg at a time, and picking replacement thrusters from the tanker.

2.9 Initial Design of the TFF craft

These craft are essentially pieces of an electromagnetic Fabry-Perot Resonator. They incorporate conducting grids spaced at a small fraction of the wavelength range where they are expected to operate. Their surface shape can be modified using extensible members driven by

electric motors, also used in their deployment in space. Two such craft would form the resonator ends, while the others would form an enclosure during the buildup of the field until the particles are already at stable locations. Following that, one wall can move away and accommodate a sintering arm from a Rockbreaker.

Each of the four sides of the resonator is sent to the construction location from Earth as an independent spacecraft which we will call a "TFF craft". Each incorporates a large (100m x 100m) thin-film microwave reflector, with a loop antenna in the middle. The power conversion equipment to generate microwaves of the required power, account for most of the mass of the craft. In the implementation developed by PSICorp[9], the conversion proceeds from solar cell to DC current, and thence through a set of vacuum devices to microwave frequencies ("Vacuum tubes" is not appropriate because the environment is a more perfect vacuum than any created on earth). The power comes from solar energy. In the initial realization of this craft, a 1 square-kilometer array of 10% efficient solar cells was considered as the power source. Recently, PSICorp[24] has refined this to a projection of between 28 and 42 percent efficiency by Year 2050, giving an array area of 0.93 to 0.68 sq. km respectively. Taking the lower limit of efficiency, we get an array mass of 472 tons, so that each craft has to carry a 118-ton array. The substrates of the solar arrays pose a huge mass penalty, which puts the system mass too high. Figure 2.5 shows a PSI design, where the entire power comes from a single panel, and the resonator is an integral box. In later designs, we chose to use four essentially identical pieces, as shown in Figure 2.3.

2.10 High-intensity Solar Cells and Concentrator

In a second iteration, the solar array was replaced with a much smaller array of high-intensity solar cells. A concentrator made of ultra-light material was conceived as the way to capture a square km of solar power and focus it onto the high-intensity array. Arrays with peak temperatures over 3000K have been demonstrated in the laboratory, which also minimize the need for other heat radiators.

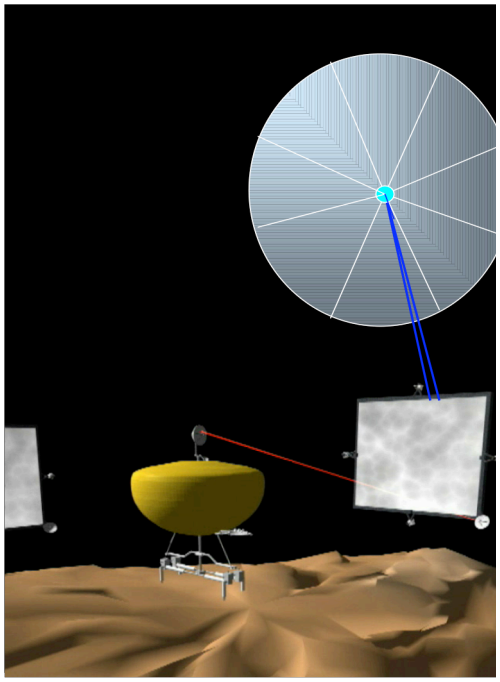

Figure 2-6: : Artist's conception of a TFF craft beaming power to a Rockbreaker about to rendezwous with a NEO. Art by Waqar Zaidi

The high-intensity array was seen as a placeholder concept, to be used until an effective direct conversion system for solar power to microwave was developed. Such a device now appears possible, given the recent demonstration[10] of a high-efficiency converter from direct sunlight to visible laser wavelengths, with a claimed efficiency of 38%. Since it is not yet possible to estimate the mass of such a device at the scale required for the TFF craft, the high-intensity array is used as an upper-bound mass estimate. Assuming a10-fold intensification the array mass per craft comes down to 11,800 kg. The rest of the craft has a mass of only 4600 kg, giving a total mass of the TFF components of 16,400 kg. This leaves 13,600 kg of subsystems for propulsion, control, communications and other items, to bring the craft mass within a 30,000kg target at escape from Earth orbit.

In these implementations of the architecture, the Rockbreaker craft would not carry their own primary power arrays for the rock-cutting operation. Instead, they would depend on beamed power from the TFF craft. This of course posed tough tracking challenges.

2.11 Integrated Solar Sail Primary Propulsion and Power Collection: Design Sizing

Given the need for a solar concentrator, solar sail propulsion is attractive. It was realized that the size of the sail required for the power focusing application is of the same order of magnitude as that needed for propulsion. ***Thus the design was driven by the sail size needed for propulsion, within***

the near solar system, understanding that this provided a large reserve of power for the TFF and Rockbreaker operations. The use of solar sails greatly reduced mission mass, since there is no need to carry ion engines and propellant, except for maneuvering.

A sample NEO rendezvous study shows that the transit time to NEO 1996-FG3 is on the order of 2 years, using a solar sail mission[11]. Rangedera et al[12] extrapolated the results of this study to design a mission concept to send a solar-sailed craft in the 38,000 kg class to this NEO. 1996-FG3 has an orbit that reaches close to the orbit of Venus at perigee, and about 2/3 of the way to Mars from Earth at Apogee. The sail size required is .51 km^2 using nested solar sails. This large size allows the sail to serve as a power system as well as the primary thrust system in the cruise leg of the transfer. The transfer to the 1996FG3 orbit is a spiral orbit characteristic of low thrust missions. The Rockbreaker mass breakdown is given in Rangedera et al and showed that the sail system could be developed well within the above propulsion system mass allotment, for both the TFF craft and the Rockbreaker. A single TFF craft with its solar collector/sail is shown schematically in Fig. 8, beaming power to a Rockbreaker.

2.12 Direct Solar Laser: Pathway to the Evolutionary Architecture

The Direct Solar Conversion Laser mentioned above (Ref. 24), enables a breakthrough. ***This laser is very similar in basic operation to the Nd Fiber Lasers envisioned as the primary cutting devices in the Rockbreaker***. The lasing wavelength is also the same, so it may be confidently integrated into the cutter systems. Now the power conversion system from solar-electric DC to the AC needed for the laser, may be replaced with the direct-conversion laser, with some marginal power converted for the plasmajet etc. Part of the stagnation temperature needed for the plasmajet could come directly from the waste heat of the direct laser conversion. ***With the direct conversion laser, the RockBreaker becomes independent of the TFF craft***. The solar sail would have to be carried with the Rockbreaker, and perhaps tethered to the NEO in case of rotation. This decoupling of the TFF craft and the Rockbreaker is a very important realization, as we proceed to the Evolutionary Architecture.

2.13 Remaining Obstacles to the DMA

Table 5 lists some of the technologies needed for the Direct Mission Architecture, and Table 6 lists the steps. The DMS architecture is definitely long-term, and poses substantial engineering challenges.

- The requirement to build the entire shell structure in one continuous operation, poses daunting robotics challenges of maneuvering, visual quality control, precise positioning and control of sintering probes and an intricate tracking to position the TFF resonator around the Rockbreaker's output spiral cloud of rubble, while also tracking the sun with one or more solar collectors.
- The Rockbreaker craft will require resupply of plasma thruster gas and replacement of solid plasma thrusters.
- The interior and the attachments of the station modules will have to be accomplished by robotic missions following the construction machines. This architecture is similar in philosophy to building an entire system of habitats, at a very low per-unit cost. The overall requirement of Earth-launch missions is summarized in Table 6.
- Finally, it is not clear if a suitable non-rotating NEO of appropriate composition can be found, with an orbit that can be reached with reasonable delta-v and mission time.
- Once the massive shell is built, further propulsion will be needed to bring it to a useful orbit.
- While none of these is a show-stopper, this architecture only becomes viable when there is a need to produce a series of large modules.

Table 2.5 : Technology development

	Demonstrated	20 yr projection
Solar Sail	Aereal density[13]: COSMOS-1 600sqm/100kg	Target[14] 0.1g/m^2
Ion Propulsion	~ 1N; T/W ~0.001	Improvement in thrust.
Nuclear Propulsion	RTDs	Thermal
Robotic Operations	Remote power plants on earth; Mars; Titan	Lunar, Martian, NEO robots
Beamed Microwave	Efficiency 0.5; 140GHz	200GHz; efficiency 0.8
Laser Cutter	10KW, 30% efficient Nd-fiber industrial use[15].	100KW
Cutting Nozzles for vacuum	Aerospike nozzles demonstrated on X-33. Plasmajet cutting used in industry.	Mature commercial technology
Direct solar conversion	38% efficient direct solar-conversion to Nd-Cr fiber laser demonstrated[10]	39% direct solar conversion efficiency
Plasma Beam	Industrial use	mature
Food growth	STS experiments	ISS and lunar base expts.
RF resonators	Military systems for RF weapons	High intensity RF common.
Vacuum devices	Large RF systems. PSICorp designs[9]	Used with solar power satellites.
Solar sails	Aereal density[16]: COSMOS-1 600sqm/100kg	Target[17] 0.1g/m^2
Ultralight booms	ISS experience, solar sail work	
In-space robotic refueling	Re-boost packages being developed; DARPA studies in-space refueling	Spacecraft routinely refueled.
Robotic sintering	Powder sintering studies for low-mass heat shields. Robotic drilling and welding in auto industry; NASA Mars drilling experiment	Feasible

Table 2.6: Steps in the Direct Mission Architecture	
Step	**Years from decision**
CaLV launch #1 sends 2 Model scale TFF craft with sample rocks to high earth orbit for system proof experiment	10
CaLV launch #2 carries 2 full-scale RockBreaker Craft to LEO / earth escape Each sends two 38,000kg craft to earth escape velocity Each craft uses Reconfigurable Solar Collector as sail to NEO Rendezvous using plasma thrusters	12
First two craft reach NEO and prove rendezvous and operations.	14
CaLV Launch #3: 1st set of 2 resonators, each 38,000 kg payload, to NEO by RCS	12
CaLV Launch #4: 2nd set of 2 resonators, each 38,000 kg payload, to NEO by RCS	12
CaLV Launch #5: 3rd set of 2 resonators, each 38,000 kg payload, to NEO by RCS. Two CaLV launches held in reserve. Estimated launch cost: $20B + $8B reserve.	15

Table 2.7: Comparison of DMA with current space projects

Task / Requirement	Comparison to current projects/ technologies
Total of 500,000 kg to LEO in ~ 10 to 20 cargo launches including mission testing. Final Construction System ~ 200,000 kg at Earth escape	ISS ~ 187,000 kg to-date
Robotics	ISS robotic arm; Mars rovers.
NEO rendezvous	Hayabusa mission
NEO Cutting	NEAP mission
Final Station assembly	ISS-scale station robotic assembly; TransHab inflatable module deployment

2.14 Economic Evolution Architecture (EEA)

The Economic Evolution Architecture adopts a strategy of waiting for the development of infrastructure in Space, through a progression from today's large projects. TFF would seek a variety of small applications, and thus solve the technical problems gradually. Thus there is little risk involved, and no technology is developed specifically for long-term human habitats.

a. TFF technology would be first put to use through several science missions, covering a wide range of applications. The technology of these applications will be developed through flight experiments, including those on the ISS or an equivalent orbital facility. Thus, this stage requires partial occupancy of approximately 5 human-carrying / resupply launches to the ISS.

b. The next step would be to set up an orbital manufacturing station, where lunar materials and earth-launched materials/ instrumentation would be combined into structural elements and machine parts with unique properties. Such a station would take as much in earth launch as the Mir station for construction, even if human presence is minimal on them.

c. The orbital manufacturing station would most probably be constructed from rocket parts such as expended fuel tanks and upper stages. This is a mechanical rendezvous and robotic construction operation, that can be performed by telepresence from Earth. It poses no serious technological challenge. However, this is likely to take the equivalent of two CaLV launches.

d. Following this, various useful parts and machines would be assembled in orbit for delivery to the lunar surface or other spacecraft, gradually expanding the capabilities. Clearly this presupposes a routine, low-cost orbital transfer tug in the Earth-Moon system, presumably a commercial operation with competition and redundancies. It also assumes that there is a market for manufactured products on the Lunar surface. Manufacturing facilities in orbit make sense because the delta-v required to get there is less than that needed to get to the Moon, and so is that for delivery to Earth markets. Launching raw materials from the Moon is not nearly as expensive, given efficient lunar launcher systems such as mass drivers. The establishment of this capability is likely to be combined with the establishment of other such orbital facilities, however, its marginal requirement for launches is estimated at 2 CaLVs.

e. The first in-space stations made primarily of lunar materials will be constructed, with high-strength skeletal structure and inflatable shells strengthened with spray-dried materials, then filled with regolith, hydrogen or water for radiation protection. This operation will be high-profile, and require as much earth-launched mass as ISS, since it is the radiation-shielding that is primarily being provided from elsewhere.

The outstanding disadvantage of the EEA is that there is no movement towards enabling delivery of large mass from beyond earth. Dependence on earth-launched mass negates any possibility of reaching the ability to build large orbiting habitats. While there may be excellent business plans for TFF along this route, none of them will lead to the primary objective of TFF, which is to form massive structures.

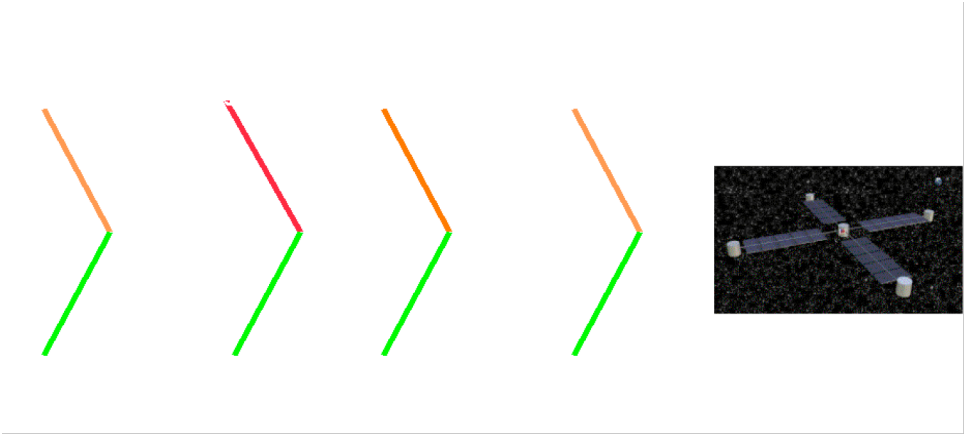

Figure 2-7 Technologies involved in developing Tailored Force Fields concept

Figure 2-7 is a fishbone diagram illustrating the primary technologies involved. Those along the lower half are all parts of the present Space program, or other NIAC concepts developments. The plasmajet cutter application is not directly involved in the Space program, but is related to plasma thruster technology which is of intense interest in the Space program. In this area, developments from the space propulsion application can be used to advance cutting tool efficiency to enable resource exploitation from NEOs. Thus all of these are marked "Green" since their development may be expected to proceed independent of the TFF program.

The technologies along the upper half of the fishbone are much more specific to the TFF program. The first is the TFF technology itself. Second is Direct Power Conversion, which appears to offer great promise in reducing the mass of equipment needed to obtain energy at desired microwave or radio wave frequencies from broadband sunlight.

2.15 References

[1] McConaghy, T.T., Landau, D.F., Yam, C.H., Longuski, J.M., "Notable Two-Synodic-Period Earth-Mars Cycler" Journal of Spacecraft and Rockets, Vol.43, No.2, March-April 2006, p. 456

[2] "Alternatives to the ESAS". http://forum.nasaspaceflight.com/forums/thread-view.asp?tid=2320&posts=83&start=1 Viewed May 28, 2006

[3] Space Studies Board: "Systems for Nuclear Auxiliary Power Reactor 1959-71" In Priorities in Space Science Enabled by Nuclear Power and Propulsion, National Academies Press, 2006, p.112

[4] Ignatiev, A., Freundlich, A., Horton, C., "Electric Power Development on the Moon from In-Situ Lunar Resources". http://www.spaceagepub.com/pdfs/Ignatiev.pdf (viewed June 1, 2006)

[5] Williams, D.R., "Luna 21/Lunokhod 2, NSSDC ID: 1973-001A". http://nssdc.gsfc.nasa.gov/database/MasterCatalog?sc=1973-001A (viewed June 1, 2006)

[6] NASA, Mars Exploration Rover Mission". Jet Propulsion Laborator, California Institute of Technology, http://marsrovers.nasa.gov/home/ (viewed June 1, 2006)

[7] Foreign Press Center, Japan: "Japan Rejoices as its Space Probe Makes Apparently Successful Landing on an Asteroid 300 Million Kilometers Distant", Science and Technology, November 29 , 2005. http://www.fpcj.jp/e/mres/japanbrief/jb_591.html (viewed June 1, 2006)

[8] Vanmali, R., Tomlinson, B., Li, B., Wanis, S., Komerath, N., "Engineering a Space Based Construction Robot", Paper 05WAC-47 (2005-01-3406) SAE World Aerospace Congress, 2005

[9] Agassounon, W.B., Crowe, D.G., Joshi, P.B., Magill, J.C., "Tailored Force Fields for Space-Based Construction NIAC Phase 2 Georgia Tech Subcontract Final Report P.O. No. E-16-X04-S1" PSI-1455/ TR-2019, June 2006.

[10] Saiki, T., Uchida, S., Motokoshi, S., Imasaki, K., Nakatsuka, M., Nagayama, M., Saito, Y., Niino, M., Mori, M., "Development of Solar-Pumped Lasers for Space Solar Power Station". IAC-05-C3.4-D2.8.09, IAC2005, Fukuoka, Japan, October 2005.

[11] Dachwald, Bernd. "Evolutionary Neurocontrol: A Smart Method for Global Optimization of Low-Thrust Trajectories" AIAA/AAS Astrodynamics Specialist Conference, Providence,RI, Aug. 19, 2004.

[12] Rangedera, T., Vanmali, R., Shah, N., Zaidi, W., Komerath, N., "A Solar-Powered Near Earth Object Resource Extractor". Proceedings of the Space Systems Design Conference, Georgia Institute of Technology, Atlanta, GA, Nov. 2005

[13] The Planetary Society, Basic Facts on Cosmos I and Solar Sailing". http://www.planetary.org/programs/projects/innovative_technologies/solar_sailing/facts.html Viewed May 28, 2006

[14] "Researchers produce strong, transparent carbon nanotube sheets" Nanotechnology, August 18, 2005. Physorg.com http://www.physorg.com/news5890.html

[15] Hecht, J., "Photonic Frontiers: High-Power Fiber Lasers" Laser FocusWorld, Aug. 2005. http://lfw.pennnet.com/Articles/Article_Display.cfm?Section=ARTCL&ARTICLE_ID=234077&VERSION_NUM=4&p=12 Viewed May 29, 2006

[16] The Planetary Society, Basic Facts on Cosmos I and Solar Sailing". http://www.planetary.org/programs/projects/innovative_technologies/solar_sailing/facts.html Viewed May 28, 2006

[17] "Researchers produce strong, transparent carbon nanotube sheets" Nanotechnology, August 18, 2005. Physorg.com http://www.physorg.com/news5890.html

3 Validation of Tailored Force Field Technology

This chapter deals with the progress of TFF technology through the validation process. The technology is related to first principles, and the basis for simplified models and calculations is examined. Phenomena in acoustic, ultrasonic, optical and microwave fields are considered, and a unified understanding is developed, in the quest for an effective prediction and simulation capability. Beyond the primary forces that drive particles towards preferred locations, we see that wall formation or other shape formation depends on secondary particle-particle and particle-field interactions. Hence analytical modeling and simulation must go down at least to the level of secondary forces. The following discussion is summarized from chapters in the doctoral dissertation of Sam Wanis.

Light absorbed at or reflected off a surface is known to exert a unidirectional radiation pressure force on the surface. Many other types of wave motion also exhibit this phenomenon. Radiation forces are also experienced by objects in other electromagnetic fields and acoustic fields. Forces exerted by surface waves on a liquid, transverse wave on an elastic string[18], can all be interpreted as radiation force on targets[19]. The phenomenon goes much beyond unidirectional force. What is of particular interest here is that the force patterns can be predicted from the boundary geometry and properties of the containers, and can be used to form and hold large numbers of particles into desired shapes. These formations can be held in position while other phenomena are used to fix the particles to each other. The issues then are:

1. Generality of the phenomenon
2. How to relate desired shapes to geometry, boundary conditions and frequencies of excitation of the container
3. How to predict forces on individual particles in order to gauge their movement towards the desired shapes.
4. How to predict inter-particle forces to gauge how they will attach to each other
5. How to predict adhesion of the particles into useful permanent shapes.

To reiterate, the fact that steady forces are generated by wave fields is well-known, in some fields. The term radiation pressure was first used in electromagnetics by Maxwell which was then introduced in acoustics by Lord Rayleigh (1905)[20] as he searched for an acoustic analogue. Manipulation of individual particles in force fields is used in various devices, such as laser tweezers, electrostatic levitators, and ultrasonic resonant chambers. That numbers of particles can be drifted into given locations in a resonant chamber is known, in other fields. Formation of chains of charged particles is known in bio/genetic engineering. What was not realized is the implication that complex shapes can be formed, and used in a vast range of sizes, materials and applications including space-based construction and micro-fabrication. For our purposes, we define a force field as a region where the force on a target object varies with position only. This implies that the force field is conservative. In this paper, attention is focused on acoustic and electromagnetic wave fields, and how to use them to create force fields. The ease of confining and controlling both field types makes these attractive for construction and manufacturing.

The magnitude of the forces produced in these types of force fields is usually small compared to those in conventional fabrication tools involving mechanical contact, used in normal earth-surface gravity (1-G) environments. However, there are two regimes where gravity is not a significant factor. The first is in orbits in space, away from massive celestial objects. Here the primary gravitational force is cancelled out, and “jitter” due to intermittent passage near gravity centers is extremely small. In such an environment, even a small sustained acceleration, on the order of one-millionth of the acceleration due to gravity at earth’s surface (1 millionth of a G), is adequate to move objects slowly into stable locations. The other regime is the micro-world, where objects and distances are so small that local forces can exceed gravity by several orders of magnitude.

Focused laser beams are used in several applications to manipulate individual particles. However, another way to generate strong forces is to use a resonator, where the steady-state input wave amplitude is much smaller than the amplitude of the waves inside the resonator. In resonators, the

forces generated can typically be 3 to 5 orders of magnitude above that of the input wave, and the "stiffness" of the stable locations can be 7 orders of magnitude above that created in a single beam.

3.1 Genesis of TFF

Reduced-gravity flight experiments[21] in 1997 through 1999 provided clear evidence that particles of several different materials and random shape, placed in an acoustic resonant chamber, would form into single-particle thick walls, positioned near and parallel to the predicted nodal surfaces. Ground experiments confirmed that the wall geometry matched pressure contours of the predicted pressure field distribution.

The search for analogous behavior in electromagnetic fields took us into the field of laser tweezers. The basic knowledge in the optical frequency range, in this area, driven by the need to manipulate micro to nanometer sized objects, provided both the theoretical framework and experimental data. By juxtaposing the acoustic field results with the optical results, we developed an analogous scaling for the acceleration per unity intensity, within the simplified "Rayleigh regime" where particle size is an order of magnitude smaller than the wavelength. Studies of the interaction of electromagnetic waves with dielectric material permitted wavelengths to be extended. Within the Rayleigh scattering regime, the expressions for acoustic and electromagnetic forces on matter were found to be similar through their dependency on wavelength; scattering particle radius; energy density of the field; impedance mismatch with the host medium; and field intensity. This permitted a large extrapolation through the electromagnetic regime, to the case of very long wavelength (~100m) radio frequency (RF) and large particles, such as 20cm-size blocks of material cut out of Near Earth Objects in space. The scaling for acceleration per unity intensity permitted prediction of the power requirements for an electromagnetic resonator required to form a massive cylinder, large enough to be a habitat module, with walls thick enough to be a radiation shield in space.

In the next phase these hypotheses were validated. An identification of all the forces involved in the proof-of-concept acoustic experiments is presented. This is done through several experiments to correlate each observed behavior to forces described in the literature.

The formation of walls is not fully explained by the behavior of isolated particles in a force field. Predictions of the forces due to interaction of two particles in an acoustic resonator indicate that a simple dipole model explains particle-field interaction and particle-particle interaction. Experiments in the acoustic resonator validate this concept, and rule out other nonlinear phenomena that are unique to the acoustic field. Simulations of the field of around dielectric particles in an electromagnetic field show that a similar model applies in electromagnetic fields.

3.2 Background

3.3

As a wave collides with a particle or interface having different impedance, the momentum and energy of the wave are altered in some fashion dictated by several parameters. In general, we can say that a change in the energy of the wave takes place through any absorption process inside the particle or interface where a dissipation of energy occurs. A change in the momentum of the wave occurs as a result of scattering (i.e. refraction and reflection processes).

3.4

3.4.1 Acoustic Radiation Pressure

Acoustic radiation pressure is the net pressure exerted on a surface, or interface separating two media, by an acoustic field[22]. Nyborg[23] shows that using the terminology used in the method of successive approximations the pressure in the field can be expressed as follows: $p = p_0 + p_1 + p_2 + \cdots$. The static pressure is given by p_0 which is a zeroth-order contribution. The first order contribution given by p_1 varies harmonically in space and time at the same frequency of the source and amplitude proportional to the source amplitude. Linear acoustics is limited to the first-order term, and thus averaging over one wave period results in a zero net pressure. At higher sound intensities second-order effects given by p_2 manifest themselves. This pressure is time-independent and can therefore induce a net pressure after time averaging. This is what we call radiation pressure. The magnitude of this second-order term is proportional to the square of the source amplitude. The higher order terms

include the pressure fields that vary in time and space at integer multiples of the source frequency and with amplitudes proportional to the source amplitude squared. These terms are usually called 1st, 2nd, 3rd harmonic etc.

3.4.2 Traveling and Standing Wave Forces

The first observation of time-averaged radiation pressure was made by Kundt[24] in 1866 when he observed dust particles collecting at the pressure nodes of standing waves setup in circular ducts[25]. The force due to acoustic radiation pressure was first measured by Altberg[26]. King[27] theoretically derived forces resulting from both traveling and standing plane waves incident on a small rigid sphere. Wanis[28] showed that since traveling wave forces are a result of the instantaneous momentum change due to scattering, and standing wave forces are a result of gradients in the energy density in the wave caused by the particle. We thus categorize traveling wave forces under *scattering forces* and standing wave forces under *gradient forces* in accordance with the terminology used in optical tweezers as will be seen later.

3.4.3 Classical Derivation of Radiation Force

The conservation equations of fluid mechanics lead, with the assumption of irrotational (and hence isentropic) flow, to the unsteady potential equation for compressible flow. This leads, for zero mean flow to a wave equation relating temporal and spatial second derivatives of the field properties:

$$\nabla^2\phi - \frac{1}{c^2}\frac{\partial^2\phi}{\partial t^2} = 0 \tag{3.1}$$

where ϕ is any of the perturbation variables. This equation leads to solutions for perturbation pressure and velocity, that are periodic in time and space. A linearized form of the potential equation is amenable to solving by superposition of elementary solutions. Elementary solutions include monopoles and dipoles, which provide convenient representation of pressure fluctuations due to dilatation and shear. Applying the boundary conditions of zero velocity and zero velocity gradient at the walls yields solutions to the wave equation by separation of variables, and use of a Fourier series. This allows solution of the resonant modes and corresponding frequencies of the chamber. Excitation at these frequencies can cause the pressure amplitude in the chamber to rise to a level limited by wall and medium losses. This level may be several orders of magnitude higher than the level of the excitation. The pressure field inside a resonator for a given mode, given by its frequency, can be solved from the Helmholtz equation, obtained by substituting a time-periodic pressure fluctuation, and separating variables.

$$\nabla^2 p + \frac{\omega^2}{c^2} p = 0 \tag{3.2}$$

The acoustic radiation force on a rigid sphere placed in an inviscid fluid was obtained by King[27] by solving for the momentum transfer that results from the scattering of a small spherical particle (*ka <<1*) placed in a stationary sound wave, by integrating the total acoustic field, incident and scattered, over the surface of the sphere. In the Rayleigh regime, with acoustic wavelength-to-particle diameter ratio of 10 or more, an analytical expression exists for the scattering cross section of these particles, where only the monopole and dipole terms need be retained. We follow Wang's derivation[29] of the force induced on a small spherical particle in a plane standing wave.

For a 1D standing wave with the pressure node at x=0, the pressure field is

$$p_i = P_o \sin kx \cdot e^{-i\omega t} \tag{3.3}$$

where P_o is the pressure amplitude, k the wavenumber, and ω the angular frequency of he field. The spherical particle is placed at an arbitrary x-location X, and a spherical coordinate system (r,θ) is placed with its origin at the sphere center and $\theta=0$ coinciding with the positive x-axis. we use the identity[30],

$$e^{jkr\cos\theta} = \sum_{n=0}^{\infty} (2n+1) i^n j_n(kr) P_n(\cos\theta) \tag{3.4}$$

along with $x=X + r\cos\theta$ to describe any general point (r,θ). Substituting this and and Equation (4) into Equation (3) now have,

$$p_i = \sum_{n=0}^{\infty} (2n+1) A_n j_n(kr) P_n(\cos\theta) \tag{3.5}$$

where,

$$A_n = \frac{A}{2i} i^n \left[e^{ikx} - (-1)^n e^{-ikx} \right].$$

for the field's spatial dependence. In the above, j_n is the spherical Bessel function, and P_n is the Legendre polynomial. The scattered wave is regarded as emanating from the sphere surface S and is described by, $p_s = p_{so} e^{-i\omega t}$, where p_{so} can be described by

$$p_{so} = \sum_{n=0}^{\infty} B_n h_n^{(1)}(kr) P_n(\cos\theta),$$

(3.6)

where $h_n^{(1)}$ is the spherical Hankel function of the first kind. Adding this scattered field to the incident field we get the total field, i.e. $p_o=p_i+p_s$. The total field can then be described by, $p=p_o e^{-i\omega t}$. Applying the boundary conditions on the surface of the sphere,

$$\left(\frac{\partial p_i}{\partial r} \right)_{r=a} = -\left(\frac{\partial p_s}{\partial r} \right)_{r=a} \tag{3.7}$$

To solve for the coefficient B_n we substitute p_i and p_s into Equation 6 and equate terms with the same n to get,

$$B_n = -\frac{(2n+1) j'_n(ka)}{h_n^{(1)'}(ka)} A_n$$

(3.8)

The last five equations provide enough information to represent the total pressure field at $r=a$,

$$p_o = \Sigma (2n+1) \left[j_n(ka) - \frac{j'_n(ka) h_n^{(1)}(ka)}{h_n^{(1)'}(ka)} \right] A_n P_n(\cos\theta) \tag{3.9}$$

Applying the small sphere condition $ka<<1$, Equation 9 becomes,

$$p_o = \left[1 - \frac{(ka)^2}{2} \right] A \sin kX + \frac{3}{2}(ka) A \cos kX P_1(\cos\theta) - \frac{5}{9}(ka)^2 A \sin kX P_2(\cos\theta) \tag{3.10}$$

Now that we have obtained the pressure field at the surface, the tangential velocity can be easily obtained, the normal velocity component being zero for rigid spheres,

$$u_\theta = \frac{3i}{2}\frac{A}{\rho_o c_o}\cos kX \sin\theta - \frac{5i}{3}\frac{(ka)A}{\rho_o c_o}\sin kX \cos\theta \sin\theta \tag{3.11}$$

The above expressions for pressure and velocity can now be used to evaluate the radiation force by substituting into the following equation described by Langevin as the basis for radiation force on a target due to an unbounded sound wave,

$$P_{Langevin} = \langle PE \rangle - \langle KE \rangle \tag{3.12}$$

where
$\langle PE \rangle = \langle p^2 \rangle / \rho_o c_o$ and $\langle KE \rangle = \rho_o \langle u \cdot u \rangle$ are the time-averaged potential and kinetic energy densities. The Langevin radiation pressure at the surface becomes,

$$\begin{aligned}\langle P_{Langevin} \rangle = \frac{A^2}{4\rho_o c_o^2}[&\sin^2 kX + \frac{3}{2}(ka)\sin 2kX \cos\theta \\ &- \frac{9}{4}\cos^2 kX \sin^2\theta + \frac{5}{2}(ka)\sin 2kX \sin^2\theta \cos\theta]\end{aligned} \tag{3. 13}$$

Thus, the Langevin radiation pressure when integrated over the surface of the sphere *S* will yield the total force,

$$F_x = -\int_s \langle P_{Langevin} \rangle \cos\theta \, dS \tag{3.14}$$

Using $dS = 2\pi a^2 \sin\theta \, d\theta$ and solving the integral from 0 to π we arrive at King's force expression (King 1934)[27],

$$F_x = -\frac{5\pi}{6}\frac{A^2 k a^3}{\rho_o c_o^2}\sin 2kX \tag{3.15}$$

Wang[22] takes this expression further and obtains a force potential, *U* from it as follows,

$$U = \frac{5\pi}{12}\frac{A^2 a^3}{\rho_o c_o^2}\cos 2kX \tag{3.16}$$

where $F=-dU/dX$. To get the traveling force expression is needed, then the above is repeated but for an incident field given by, $p_i = p_{io}e^{-i\omega t}$, where now $p_{io} = Ae^{ikx}$. When this is done the final result for the force is[27],

$$F_x = \frac{11\pi}{18}\frac{A^2 k^4 a^6}{\rho_o c_o^2} \tag{3.17}$$

The main distinction can be clearly seen that the traveling force does not have any spatial harmonic dependence as does the standing wave force, which has a spatial frequency double that of the pressure field. The higher dependency of the traveling wave forces on *ka,* being on the order of $(ka)^3$ times more, shows why standing waves produce orders of magnitude larger force for the same field intensity. This force also scales linearly with intensity and cannot be put in a form such that it depends on the gradient of the intensity as does the standing wave force. This point becomes important when the analogy between acoustic and electromagnetic force fields is considered.

3.5 Electromagnetic Forces

It is well known that electromagnetic waves carry both momentum and energy. An incoming electromagnetic wave impinging on a perfectly absorbing flat plate will exert a net radiation pressure, $P = QI/c$, where I is the beam intensity, Q is 1 for perfectly absorbing and 2 for perfectly reflecting plates, and c the speed of light. For a perfectly reflective surface the change in momentum is doubled and therefore the pressure is doubled ($Q=2$). The idea that light can exert forces on neutral matter was introduced as far back as Kepler and Newton and was not confirmed until Maxwell's equations for the propagation of electromagnetic waves were introduced. Maxwell calculated the forces to be extremely small for conventional light sources. With the advent of the laser several experiments have demonstrated the capability of manipulating micro-meter sized particles using the momentum of laser light[31]. Later, they showed that a laser beam going into or out of a dielectric liquid (i.e., water) will exert an outward radiation pressure on the interface separating the water from air, i.e. away from the water into the air.

Electromagnetism also lends itself to linear models. Maxwell's equations of electromagnetism also lead to the result that all components of the electrical field vector E and the magnetic field vector H also satisfy the same form of wave equation as given for acoustics.

3.6 Scattering and Gradient Forces

Ashkin[31] was the first to report using optical radiation pressure to trap neutral dielectric particles. The work done by Ashkin laid the foundation for much of the work on optical tweezers. Optical tweezers manipulate and trap microscopic particles via the interaction between optical fields (i.e. electromagnetic fields) and matter. Starting with Ashkin's demonstrations of using radiation pressure to guide and trap particles, optic tweezers began to gain popularity. This was expanded by the breakthrough realization that a focused light beam attracts a small particle with index of refraction higher than the host medium, towards its beam focus. The wide range of use of optic tweezers is evident from applications in trapping and cooling neutral atoms[32] to manipulating single living cells[33]. They have been used to measure elastic properties of cells and molecules[34]. Constable[35] has shown that a pair of pig-tailed (i.e., intertwined) optic fibers can be used to utilize both scattering and gradient forces to trap particles in the gap between the fiber ends. This was later used to stretch soft biological samples. The sample was being stretched due to its having a higher index of refraction than the surrounding medium. Most recently, Dholakia and McGloin[36] used laser tweezers composed of a pair of pig-tailed optic fibers to controllably push and pull trapped particles of various sizes. An excellent summary of the current state-of-the-art on manufacturing with light is given by Dholakia and McGloin. Tailoring of the light field is mentioned as a means of enhancing the capability of optical tweezers in molecular level manufacturing.

3.7 Rayleigh Regime

Analytical work by Zemanek[37] has classified trapped objects into two groups: objects having a radius larger than $\lambda/20$ where generalized Lorentz-Mie scattering theory must be applied to express the radiation forces; and objects smaller than $\lambda/20$ (Rayleigh regime) which can be modeled as electric dipoles. In Rayleigh scattering theory, the incident electric field induces an electric dipole in the dielectric particle. The oscillations of the induced dipoles radiate a scattered field that interacts with the incident field and alters the energy density of the latter. Such interaction exchanges momentum between the fields yielding a force on the dielectric particle. This is the so-called *scattering force*. The Lorenz force acting on the induced dipole is termed the *gradient force*[38].

Clearly, the mechanisms for force generation in acoustic and electromagnetic fields are different; however, they are similar when generalized to basic physical quantities such as energy density and momentum[28].

3.8 Primary Forces on Particles

The forces exerted onto a large number of particles placed in acoustic or electromagnetic fields (whether traveling or standing) can be split up into primary forces and secondary forces. Primary forces are due to the external field and are responsible for collecting the particles towards their final destination. Secondary forces are only effective at close range and are a result of the radiated field of one particle influencing the incident field of another. Primary forces dominate until two or more particles come close to each other and

then secondary forces take over. Thus, the final finishing form of the structure formed is dictated by secondary forces whereas the general overall geometry is governed by primary forces.

Based on the analogy between acoustic and electromagnetic forces a generalization was done in order to unify the force expressions[28]. This led to simplified forms of the forces generated by wave motion onto matter and is listed in the following sections.

3.9 Unified Force Expressions

The derivation of forces onto a large number of particles placed in acoustic or electromagnetic fields can be essentially broken into the following steps:

(a) Assume the particles are far enough from each other and container walls to enable resolving the force onto a single particle
(b) assume that the particle is small enough such that the incident field onto it is essentially uniform across its diameter (Rayleigh approximation)
(c) assume the particle is spherical which is a good assumption if the particle is small enough to be in the Rayleigh scattering regime
(d) we now have a classical physics problem of solving the scattering from a small sphere placed in a uniform field. The boundary conditions are applied at the sphere's surface and the field solved for inside the sphere.
(e) The total field is the superposition of the incident field and that radiated by the sphere (scattered).
(f) The force is calculated by integrating the field around the particle and taking the difference between that field and that which would have existed without the particle. We call this force type momentum-based (aka scattering forces). The other component of the force is computed by taking the –ve gradient of the total (incident and scattered) potential field, i.e. $F = -\nabla U$. We call this force-type energy density-based (aka gradient forces).

Performing the above steps for both acoustic and electromagnetic waves Wanis[28] obtains a unified force expression that can be used for both fields. For the forces based on energy density,

$$\mathbf{F} = \mathbf{V}\Theta\nabla\xi \tag{3.18}$$

Similarly, acoustic traveling wave forces and electromagnetic scattering forces were generalized into the following unified force expression – based on momentum,

$$\mathbf{F} = \left(\mathbf{k}^4\mathbf{a}^6\right)\Theta^2\left|\xi\right| \tag{3.19}$$

The main distinction between the two forces is that the gradient forces can be negative based on the sign of Θ and is proportional to the particle volume and gradient of energy density. Momentum forces are always positive (i.e. away from the field source), proportional to the particle radius to the sixth power and inversely proportional to wavelength to the fourth power, and proportional to the local field intensity.

3.10 Secondary Force Fields

In like manner to the primary forces, the secondary forces also resemble each other in the two fields in 2D. In acoustics, the force of interaction between two dipoles goes as the square of the pressure amplitude (i.e. acoustic energy density), inversely proportional to the separation distance to the fourth power. In electromagnetics, the force of interaction between two electric dipoles is proportional to the electric field amplitude squared (i.e. electric energy density) and inversely proportional to the separation distance to the fourth power. Clearly, both secondary forces are analogous, and this stems from the fact that they are both dipole-dipole interaction forces.

3.11 Difference Between Structure Formation in Acoustic and Electromagnetic Fields

The main difference between acoustic and electromagnetic dipoles comes in the regions of attraction and repulsion. In acoustics, the attraction regions are along two dimensions and repulsion along the 3rd, whereas in eletromagnetics there is only one dimension that experiences attraction, and the other two are repulsion. This behavior in acoustics and electromagnetics is illustrated below. In the force field around a small particle in a sound field is shown. The electromagnetic counterpart is the same except that the force vector directions are reversed, i.e. the repulsion zones become attractive and the attractive zones become repulsive. The net result of this on the structures formed is that in acoustics we can achieve complete surfaces that vary in 3D space by exciting one resonant mode.

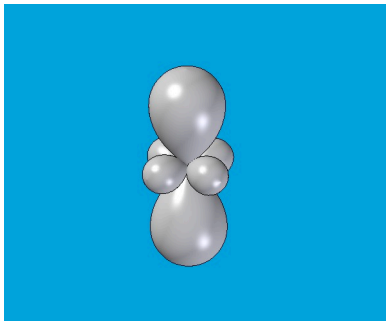

Figure 3-1: Attraction and repulsion zones in acoustic fields in 3D

Acoustics
$\mathbf{F_s} = 4\pi \mathbf{a}^6 \left[\frac{(\rho - \rho_o)^2 (3\cos^2\theta - 1)}{6\rho_o \mathbf{r}^4} \mathbf{v}^2 \right]$
Electromagnetics
$\mathbf{F_s} = \frac{\mathbf{p}_1 \cdot \mathbf{p}_2}{\mathbf{r}^4} \left[1 - 3\cos^2\theta \right]$

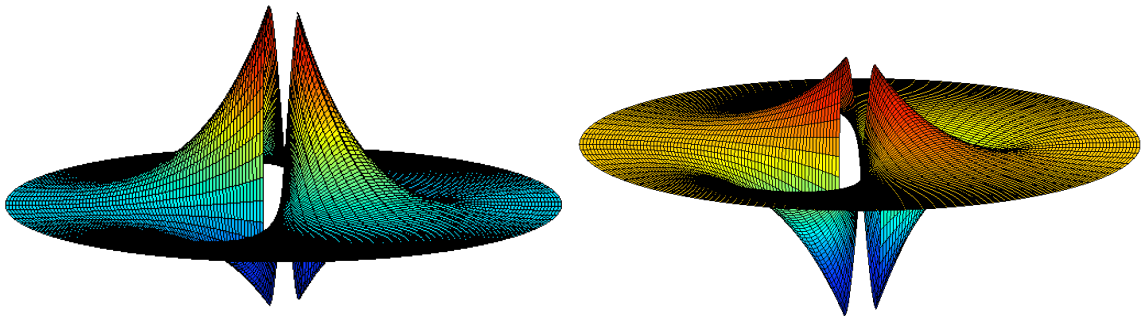

Figure 3-2:Interaction potential for two particles in acoustic fields (top) and electromagnetic fields (bottom). Height denotes potential amplitude.

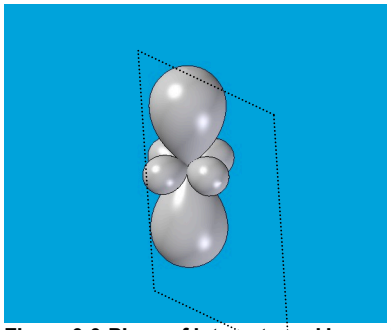

Figure 3-3:Plane of interest used in producing potential plots of Figure 3-2.

In electromagnetics we predict that since there is attraction along one dimension only, then the resulting structures are chains and not complete surfaces. These chains vary in 3D space depending on the resonant mode of excitation. To achieve complete surfaces in electormagnetics we hypothesize that a second mode needs to be excited once chains have formed and cured to force the chains to coagulate and then cure them into complete surfaces. Another difference between the two secondary force fields comes when the acoustic force has a nonzero monopole term. This is proportional to the ratio of the compressibility of the particle to the host fluid. In electromagnetics we do not see a mechanism for this to occur as long as the dielectric particle with which we are dealing does not have any net charge, and thus no electric monopole term.

The dipole equivalence of the behavior of a sound scattering particle in acoustics and a dielectric particle in electromagnetics, has been demonstrated experimentally, verified numerically, and shown analytically. Experimentally, we showed that the forces of interaction between two suspended particles in a sound field attract along one axis and repel along the other. This is characteristic of dipole-dipole interaction forces. Numerically, we solved for the field around a sound scattering sphere and a dielectric in FEMLAB and showed that the field around both spheres resembled that of a dipole. Finally, we showed that analytically, the interaction between two spheres in both fields have very analogous behavior. This is mainly because they are both regarded as dipoles in their respective fields. This is the basis of the strong analogy between the two fields. The interaction forces in acoustic and electromagnetic fields between two small particles are listed below. Figure 3-2 shows the potential energy of interaction, which when operated on by the gradient operator, yields the interaction forces. These plots represent the potential around a single particle due to the presence of another particle close by in 2D. The plane is selected such that it covers both attractive and repulsive regions as shown by the plane in Figure 3-3

3.12 Curing Fields

Heat generation from electromagnetic waves was studied as a means of surface curing by way of sintering. The physics of heating by electromagnetic waves is heavily dependent on the dispersive nature of the dielectric constant. An example of this phenomenon is the fact that white light passing through a prism becomes separated into a rainbow of colors with blue being refracted the most and red the least. This is a manifestation of the dispersive light speed in materials. Recall that the speed of light can be determined from, $c=(\varepsilon\mu)^{-1/2}$. Thus, if $c = c(\omega)$ then either the permeability μ or the permittivity ε or both are functions of ω. In practice, most materials have a permeability μ that varies very little with frequency[39]. It is the permittivity ε that can vary significantly. Equivalent elementary circuits can be used to describe this behavior as will be shown below[40].

3.13 Physical principles of heating

Electromagnetic heating is the conversion of electromagnetic energy into heat within a dielectric material. This heating technique is distinct from conventional heating, which require thermal heat-flux through heat conduction and convection, in that it is a volumetric heating technique. As a dielectric material is placed in an alternating electric field the constituents making up the material respond according to their respective charges. As described earlier, in the simple example of electrostatics, the positive charges (protons) are shifted slightly in the direction of the electric field, while the negative charges (electrons) respond by shifting slightly in the opposite direction, in other words, a collection of dipoles is induced within the materials volume. In this configuration, the particle is said to be polarized. This situation becomes complicated quickly as the external electric field becomes unsteady, i.e. starts to alternate its direction back and forth. The induced dipoles in turn respond to such field oscillations by switching their dipole moment p direction

back and forth. For a hypothetical massless ideal dipole with only two opposite charges, it is clear that this dipole would manage to maintain perfect alignment of its dipole moment p with the electric field E at infinite frequency. Now, turning to real materials, we consider the response of a single molecule located at a general point within the particle. The oscillation of its charges back and forth, or the response of the induced dipole formed within the molecule, will be in response to the local field produced at that point. The local field is affected by the neighboring molecules and their induced dipoles. It now becomes evident that the material's molecular and atomic structures plays a major role in determining the polarization behavior. It is possible that at certain frequency bandwidths the response of the material can change dramatically. The behavior of the material's constituents (i.e. charges) depends on the binding forces that hold the electrons in place. It is assumed that since the electron mass is much less than the proton mass, and that the electrons move relative to the relatively fixed nucleus). This is only adequately addressed using quantum mechanics. However, classical approaches have been used to approximate such behavior by studying the response of a mass-spring-damper system with excitation frequency[41]. In the years before quantum theory was accepted[42,43] addressed the problem of electromagnetic interaction with a particle consisting of many thousands of atoms. Rayleigh in 1871 developed an approximate analysis which is valid for very small particles. The polarization using the Clausius-Mossotti relation shown earlier is a result of the continuum theory of dielectrics.

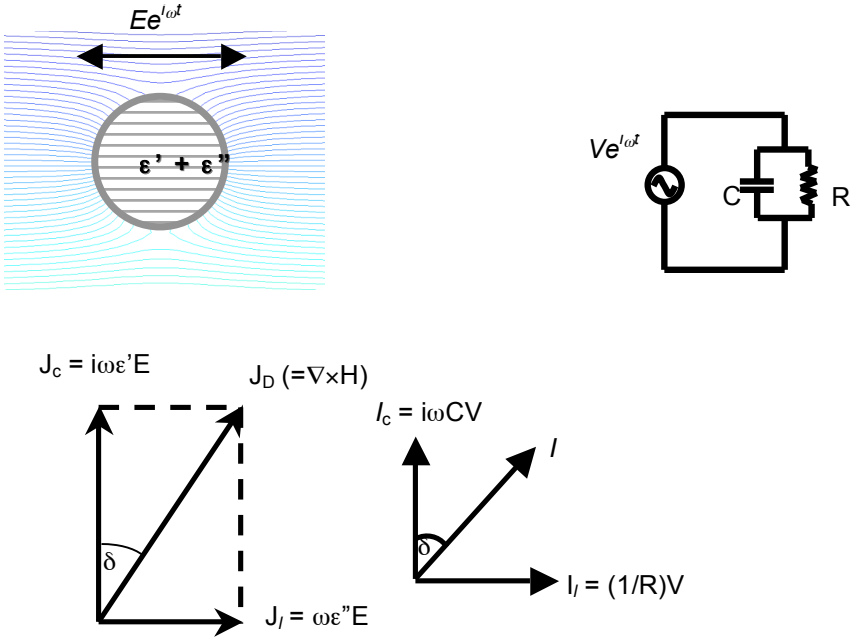

Figure 3-4:(Left) Dielectric sphere in alternating electric field and its corresponding phasor diagram where Jc is the polarization or charging displacement (i.e. electrical flux density) and JI is the loss charge. (Right) Equivalent electrical RC circuit.

For the purposes of this paper, it is enough to state that the dielectric constant is a function of frequency and can be re-written as, $\varepsilon(\omega) = \varepsilon'(\omega) + i\varepsilon"(\omega)$. The real component describes the ability of a material to polarize in response to an external electric field, whereas the imaginary component is a measure of the loss in the material. This "loss" is the mechanism by which energy in the external electric field is transferred to the material and dissipated into heat. Clearly, the part of the wave's energy density that goes into polarizing the material through ε', is stored within the particle volume U = -p·E. Ideally, the polarization process is reversible. On the other hand, the energy density that goes into the material through ε" becomes absorbed. This contributes to translational, rotational, and vibrational motion of the charges, raising the material's temperature. This energy gets dissipated throughout the volume of the particle. This is an irreversible process.

In linear systems, the response is proportional to the stimulus in equilibrium. At very low frequencies any dipoles in a medium will have enough time to match the variations of the external electric field. At this point the dielectric constant is at its maximum value since the bound charge density reaches its maximum value and energy from the external field is stored within the dielectric material. As we increase the frequency, the

dipoles are no longer able to restore their original positions during field reversals and as a consequence the polarization lags the applied external field. When the polarization lags behind the applied field there exists a component along the direction of E in phasor space as shown in **Error! Reference source not found.**. This real component gives rise to absorption of electromagnetic energy in dielectric material.

Relaxation describes the phenomena responsible for the delayed response of the system to a changing stimulus. In resistance-capacitance (RC) circuits we know that the relaxation time is simply the product *RC* (resistance times capacitance). It can be shown that $RC = \varepsilon/\sigma$. The value of ε/σ is the relaxation time where the charge deposited inside a lossy dielectric will decrease by a factor of 1/e. This is one example where the microscopic picture corresponds accurately with the more familiar macroscopic one.

The reduction of the effective polarization manifests itself as a fall in the dielectric constant and a rise in the loss factor as shown schematically in **Error! Reference source not found.** Now, energy is drawn from the field and dissipated within the dielectric as opposed to being conservatively stored in it. This dissipation of energy is the heat source that we use to raise the temperature of the particles.

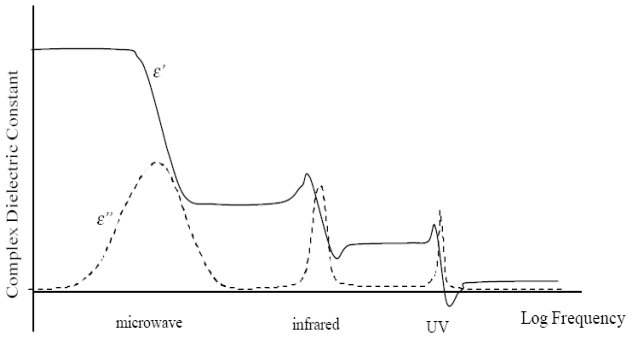

Figure 3-5:Dispersive nature of dielectric constant and loss of an ideal nonconductor

The dielectric constant is a complex number, meaning that the polarization does not follow the electric field but is shifted in phase. The frequency dependence of ε' and ε" is shown in Figure 3-5 for an ideal non-conducting material. At low frequencies, ε' is composed of contributions by all three polarization mechanisms discussed later. The dominant mechanism is the dipole orientation process. As the frequency increases the dipoles start exhibiting relaxation and are unable to respond fast enough to keep up with the imposed external alternating electric field. At this stage atomic polarization becomes the most effective polarization process induced by vibrational motions of the individual atoms in a molecule. At even higher frequencies, inter-atomic vibrations cannot respond fast enough and give way to electronic oscillations, which now become excited. This typically occurs around the UV region of the spectrum. Finally, as the frequency continues to increase, we reach a point where all electronic modes are exhausted and ε' approaches unity. It is clear from Fig. 3-5 that wherever ε' changes most dramatically there is an associated peak in ε", which characterizes the absorption of radiation by the dielectric. This absorption arises from the resonances associated with vibrations of atoms and molecules composing the material. In solids, the molecules are close enough that significant interactions occur between them. The internal modes of oscillation are therefore modified and the natural frequencies of the atomic oscillations are spread out by the interactions producing a broadening of the absorption lines. This is also referred to as dispersion. This means that instead of well defined characteristic energy levels associated with molecular vibrational and rotational states there will now be a more continuum band of energy levels. Since energy bands in solids are sums of the energy levels of individual molecules, the spectral positions of the more continuous absorption bands overlap the absorption spectrum of individual molecules. This is important when considering scattering from an object. For example, the electrons in a given material have an overlapping continuous distribution of energy levels. If one of the overlapping bands is partially empty and an electric field is applied, then it will be able to excite electrons into adjacent unoccupied states. This is how an electric current is produced in a conducting material under the application of an alternating electric field.

3.14 Temperature change

Starting from conservation of energy and following Metaxas' derivation[44], we get the time rate of change in temperature given by

$$\frac{dT}{dt} = \frac{\frac{1}{2}\omega\varepsilon_o\varepsilon''|E|^2}{\rho_o c} \tag{3.20}$$

Solving for the average power dissipated within a dielectric of volume V results in the following, expressed in W/m^3:

$$P_{dis} = \frac{1}{2}\varepsilon_o\varepsilon''V\omega|E|^2 \tag{3.21}$$

3.15 Surface Formation and Curing Process

Based on the data for a perfect dielectric, it became evident that the frequencies that we would use for pushing particles to their equilibrium positions (gradient and scattering forces) can be widely separated from the frequencies that we use to heat up the surface once the shape is formed. This finding (which may not be true in all regimes of particle size, structure size and material properties) allows us to decouple the two fields from each other since they have different frequencies: one for shaping and the other for heating[45]. A schematic showing a rough estimate of the frequency selection for both stages of the large-scale space structure construction process is shown in Table 3-1. The middle frequency band will be used for refine positioning of any stray particles that have drifted away. At these smaller wavelengths compared to the shaping field wavelength the forces are higher albeit very directional. However, the possibility remains of finding microwave frequencies that may heat up specific materials, within the construction band. This opens possibilities[46].

Table 3-1: Frequency spacing of each step of the electromagnetic construction process

Process	Frequency Range	Spectrum Segment
Shaping	0.1 to 100m	Low RF
Refinement	10 to 100mm	Microwave
Heating & Curing	1 to 100 microns	Infrared/high microwave

3.16 Application to Space Based Construction

In the zero gravity environment of space small forces produced by waves can achieve significant results. The acoustic wall formation process has been validated by reduced-gravity flight experiments as discussed earlier. However, acoustic fields imply use of a liquid or gas medium, and hence a pressurized enclosure. The dimensions of this enclosure will be limited by the wavelengths that can be generated, and the mass of the enclosure and medium. Thus acoustic manufacturing in Space is attractive for forming objects in the range of 0.01 to 10m.

The problem of radiation shielding rules out low-mass structures for human habitats. Radiation in the solar system consists of particles, gamma rays and X-rays from the sun, along with high-energy particles such as cosmic rays[47]. Hydrogen, water and polymers must be shipped from Earth, which increase the launch mass required which in turn translates into higher and higher launch costs. An attractive option, if feasible, is to use material from extraterrestrial, low-gravity sources, with minimal processing, and simply provide a thick, dense layer of mass that stops all forms of radiation. The thumb rule is that a layer of soil 0.5 m thick[48] would provide complete protection. The construction process cannot require human presence for long durations.

In order to size the power requirements of a full-scale construction system, an estimation method had to be devised for the forces that could be generated in fields large enough to be applied in large-scale construction. The key issue is to see what power levels are needed in order to achieve a given acceleration level on solid particles of a given size, using a given wavelength. The wavelength is dictated by the mode

shape needed to construct walls of a given curvature. For a full-scale habitat module, the module size was estimated to be a cylinder 50 m in diameter and 50 m long. The sizing criterion used here was the amount of space afforded to large animals that live in captive but comfortable environs for many years in the better Zoological gardens – this is more representative of requirements for long-term human habitation than the present generation of "space stations" and "crew vehicles". Four of these modules tied with tensile tubes to a fifth module at the center, would form a habitat station with artificial gravity in the outlying modules, and zero gravity inside the center module. The particle size needed for construction is chosen to be practical for material handling and to keep the formation time of the module within reasonable limits. As long as the acceleration caused by the field is larger than that due to the other random or systematic "g-jitter" in the construction region, then it may be assumed that the field will be successful in driving the particles to stable regions and holding them there until they are fused in position. If the power required to achieve this acceleration is feasible to develop, then the construction scheme can be developed further.

3.17 Sizing Metric: Acceleration per Unit Intensity

In order to start the process of conceptual design for construction on this scale, a way had to be found to extrapolate the results found in the literature. For this a suitable metric is the acceleration per unit intensity, to be expected in a given size regime and wavelength regime, for given type (acoustic, optic or microwave) of force fields. To compare these forces, a substance had to be found that can be manipulated using acoustic, optical, and longer-wave electromagnetic fields. Figure 3-6 shows results calculated for silicon dioxide. The density was approximately the same for the forms used in all types of fields, though the form varied. The ratio between particle size and wavelength was held constant at 10 in order to use Rayleigh regime results. We used the following logic to enable a direct comparison of different types of waves and particles, drawing upon each application area. Silicon dioxide in glass bead form is transparent to laser light and RF, and can also be manipulated using acoustic fields. The force per unit incident radiation intensity is divided by the mass of a particle to obtain the acceleration per unit intensity. The abscissa is the particle radius. The corresponding pressure field amplitude and electric field amplitude were then calculated.

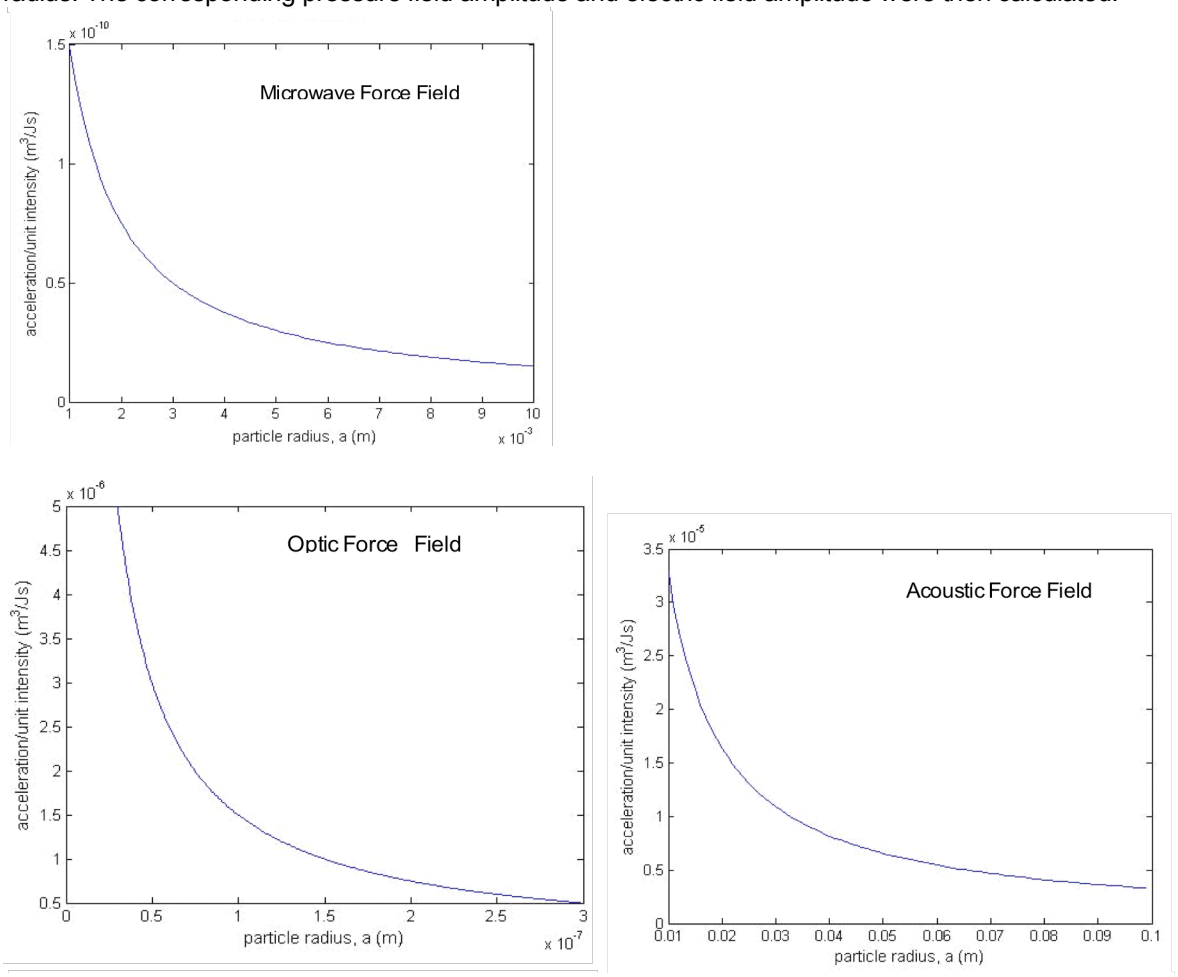

Figure 3-6: Acceleration per unit intensity for three force fields

3.18 Process for Space-Based Construction and Manufacturing

The manner in which structures could be constructed in space using TFF is as follows:
The construction material is broken up into appropriate size range particles.
The unsteady potential field best suited for the size scale of the object is selected.
A resonant field is setup by adjusting the field source frequency or the dimensions of the boundaries or some combination of the two.
The construction material particles now respond to the radiation pressure imposed on them by scattering the incident wave and, altering the wave's momentum path. They thus react by moving to force nodal locations within the field. In other words, the particles are attracted to points of minimum potential in order to minimize the total energy of the system.
Once stable, a suitable curing method is employed to fuse the particles together forming a permanent structure. Since chains form in electromagnetic force fields this may be repeated several times in order to obtain a solid surface out of the chains formed in the initial shaping process.
If the final object consists of many smaller objects, i.e. span a large size scale, then individual structures could be fabricated using this force field method and final assembly would occur externally via any appropriate means, such as a robot.

3.19 Architecture Choices for Space-Based Construction

Given the result above, that electromagnetic fields can be used to build chains, rods and other detailed structural components, it is clear that electromagnetic fields are better used to build components, rather than assemble large walls. The NEO material extraction technique described there, was based on sending a robotic Rockbreaker craft which was propelled by a solar sail. The craft instead used beamed power from a solar power converter on one of the construction craft. This was driven by the mass of the system required to convert solar power to useful electric power. The Rockbreaker used Neodymium fiber lasers to cut NEO material.

The direct solar-pumped ND fiber laser described by JAXA[49] opened the way to separating the construction and rock-breaking parts of the habitat construction mission. Now the solar sail / collectors on the Rockbreaker can be used to directly pump the lasers used in the rock-cutting[50].

In turn, this implies that there is no need to do the construction at the NEO. Instead, the material cut from the NEO can be collected and shipped back to Earth orbit using solar sails. Since the material is confined, it poses no debris threat. The material can instead be sorted and processed to extract different resources, before the remaining material is used to form structural components[51].

A simple conceptual design for a Space Manufacturing / construction facility could be based on Space Shuttle External Main Tanks, or comparable large expendable fuel tanks used by heavy launchers. The interior could be configured into acoustic or electromagnetic manufacturing chambers. The acoustic chambers would be used to form walls, panels and tanks of specified shape. The electromagnetic chambers would form linear elements such as beams and rails. Being in Earth orbit, telepresence can be used to control the processes.

3.20 Summary of Validation Points

The prospect of tailoring potential fields for automatic, large-scale space-based construction was presented in 1999[52], and has been followed up through several papers. The current validation status of the basic phenomenon is first summarized. The fundamental phenomenon behind force-field tailoring is the force generated on objects placed within a resonator, driving them to stable locations where they organize into walls or chains. It was first shown using acoustic fields, but then extended to electromagnetic fields covering a wide range of wavelengths, particle sizes and material characteristics. While some organization of material, and even some wall formation, can be seen in experiments conducted in the 1-G environment, wall formation becomes a primary feature of particle behavior when gravity is removed. Starting with reduced-gravity flight tests on the NASA KC-135 Reduced Gravity Flight Laboratory using an acoustic

resonator in 1997, we have shown the following through flight and ground experiments, and by reference to the work of others on different applications:

3.20.1 Reduced-Gravity Flight Test Results

a. Solid partices of arbitrary shape form **walls** near the nodal surfaces of a resonant sound field[53] when the particle size is much smaller than the wavelength (the Rayleigh regime. This is different from the well-known experiments on "acoustic levitation" which have been carried into experiments on the STS. In those experiments, the effort was to position and hold a single particle, in the ultrasonic regime where the wavelength is of the same order of magnitude as the particle diameter (Mie regime), and very high intensity is used. It is also different from the "fingers of sound" approach where again the particles are in the Mie regime, and distinct beams of ultrasound are controlled to manipulate discrete particles.
b. Materials with widely different properties and shapes, including dielectrics and metals, form walls at the same locations[54]. Thus suspicions about static electricity etc. are removed.
c. The wall formation does not depend on streaming or other phenomena unique to acoustics[55]. In fact it works better with low intensity of sound, where streaming is not an issue, provided there is only low frequency, low-amplitude g-jitter[54].

3.20.2 Ground test results

d. The walls form at or near the predicted nodal surfaces from the solution of the Helmholtz equation for a resonator.
e. Complex wall shapes are predicted from simultaneous excitation of multiple modes, and evidence of these shapes is seen in traces on the floor of the resonator in 1-G ground experiments. However, these are too fragile to be seen clearly during the short durations of clean microgravity available in KC-135 flights.

3.20.3 Early Implications

The reduced- gravity flight experiments demonstrated the potential for non-contact shape formation in space using acoustic fields and randomly-shaped particles. However, this is limited to objects on maximum size on the scale of 1 meter, by the need for a closed, gas-filled container, and the longest wavelengths at which an acoustic field could be made to resonate. To build massive radiation shields in space, it was necessary to take the technology to a much wider range of wavelengths. For this, we investigated the possibility of generalized force fields, and specifically, electromagnetic fields.

3.20.4 Theory and experiments from the literature

f. Previous work in the literature, under various technology areas, has shown the following:

g. The forces are generated due to scattering of the waves by particles[56]. This basic idea has been known and quantified since the work of King in 1935.
h. Theory for optical tweezers and laser microscopes describes force generation mechanisms in the nanometer to micrometer size range. This is analogous to those seen in acoustics and ultrasonics, and analogous relations can be developed[57].
i. The radiation force thus generated is amplified by several orders of magnitude in a resonator, and the wall locations have high "stiffness" and stability[57].

j. The equations describing the generation of such forces in acoustics and electromagnetics are similar in form, and analogous relations were developed[58]. This has been linked back to first principles in the PhD dissertation work of the second author[59].

3.20.5 Scaling to Large-Scale Space-Based Construction

A rudimentary scaling for the acceleration per unit field intensity was developed from this analogy and extrapolated into the radio frequency (RF) regime[58]. Using this scaling, we predicted the design parameters

for a 50m diameter, 50m long cylinder with walls 2m thick – enough to stop any radiation expected in Space at the orbit of Earth around the Sun (1 A.U.). The recent standard NASA reference on radiation shielding[60], gives the required shield thickness of regolith as only 0.5m, greatly simplifying the construction problem and slashing the energy requirement and the time taken to extract material and build the structure. The required solar power was estimated, to generate a long-wave radio frequency (RF) field strong enough to cause a 1 micro-g acceleration on 20cm blocks of material of specific gravity 2.0 (similar to earth soil), driving them towards the stable wall locations. The wall locations themselves are stable. The point of this exercise was to check the magnitude of power input needed in a resonator to form rocks into a cylindrical wall, and relate this power to the size of a solar array required at 1 A.U. It turned out that the area of the solar array was large, but not unreasonable – on the order of 1 square kilometer at 10% efficiency. It was recognized that the 50m dimension, the 2m wall thickness, and the 10% solar cell efficiency, were all probably far from values for an optimized space station module and a construction system; however, they were chosen to be conservative limits in order to check the upper bound energy requirements. The technical challenge at this point was to validate the extrapolation of the analogy between acoustics and electromagnetics, to wavelengths and particle sizes far beyond the micron range of laser optics and optical tweezers.

k. The electromagnetic force on a single particle measured in a microwave resonator in an experiment conducted by the Jet Propulsion Laboratory[61] is successfully and accurately predicted by the scaling relations developed from the acoustics-electromagnetics analogy[62]. Thus at this writing, experimental validation has confirmed the force expressions for a single particle of specified dielectric properties in an electromagnetic field, at the millimeter scale of particle size, in a microwave field, operating at the border between the Rayleigh regime (particle size << wavelength) and Mie scattering (particle size ~ wavelength).
l. Thus the scaling is seen to hold over the size range from nanometers to several millimeters, and from wavelengths of sub-micrometer to centimeters. Our postulate is that it can also be extended to particle sizes of several centimeters, and wavelengths of 100 meters.

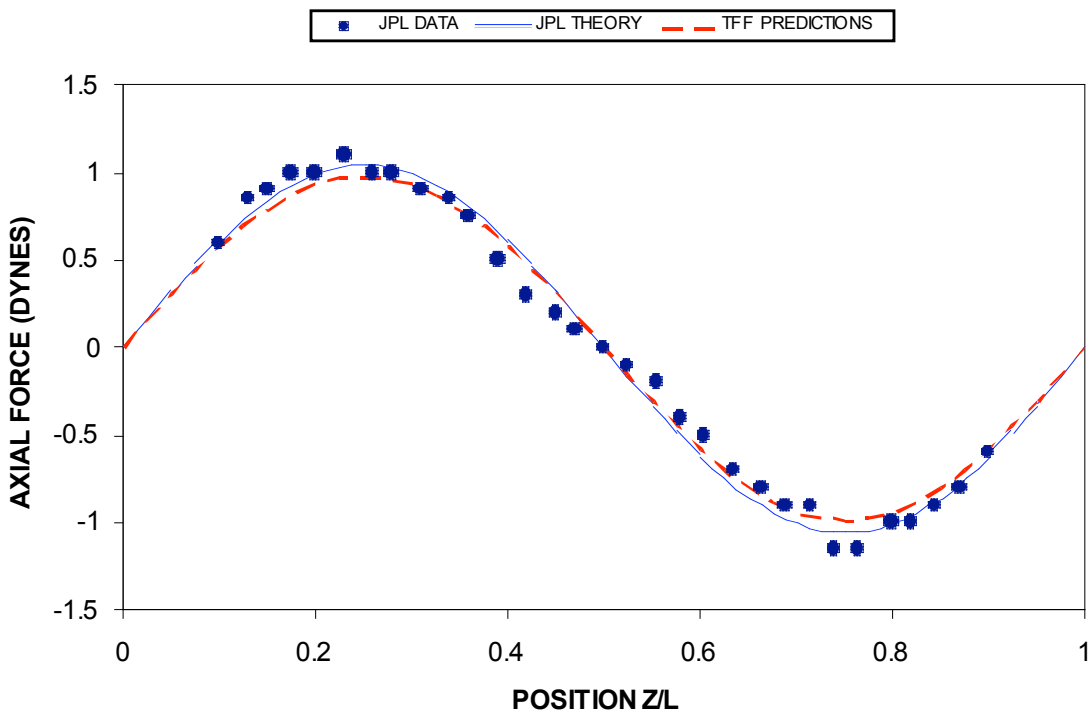

Figure 3-7: Force on a single object in a resonant microwave cavity. Resonant mode is TE11. Frequency is 4.84GHz, source power 20 watts, resonance Q factor is 6100, sphere diameter 9.4mm and dielectric constant is 11.

The above represents the state of knowledge that existed to drive the initial conceptual design of how to construct a large station. Only walls were believed to be formed. Since low-gravity quarries for raw material implied Near Earth Objects or asteroids, and the wall formation process would be imperfect, releasing

blocks of material into space, the process was not considered suitable for implementation near Earth, as it might generate possible space debris hazards. The construction was thus believed to be restricted to locations far from earth, and the Earth-Sun Lagrangian Point L-4 (ahead of Earth in its orbit around the sun by 60 degrees, or two months) was envisaged as a possible location for the first construction station. Objects at this location are stable to small perturbations, and hence require minimal station-keeping fuel. This location also offered a convenient reference point, since the solar radiation, and the solar energy density, were the same as those immediately outside Earth's magnetic field. Two subsequent (recent) realizations are summarized below.

m. While the radiation force that drives particles towards preferred surfaces in the resonant field is analogous between acoustic and electromagnetic fields, and scaling for power presented above is valid, the wall formation process is quite different. This difference merits a separate discussion below.

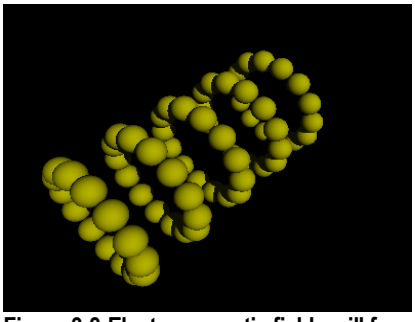

Figure 3-8:Electromagnetic fields will form chains rather than the walls shown forming in a reduced gravity flight test in an acoustic field.

n. Wanis[59] has developed, through physical and numerical experiments, a consistent model for self-organization of particles in resonant standing wave fields. The implication his work is that in acoustic fields, particles will self-organize along surfaces, and form walls one particle thick, but further control within the surface is difficult. In an acoustic standing wave field, particles drift towards nodal surfaces. In electromagnetic fields, however, self-organization can be taken to one level finer in control. Particles can be aligned and joined together along specified lines, forming chains or rigid links of desired shape. This is illustrated in Fig. 1. Once the chain is fused together, it can be treated as a single particle, and other chains or particles can now be attached to it, depending on its orientation.

The implications are that:

o. By turning the field direction, these elements can then be combined to form more and more complex structures.

p. ii. By changing wavelength, the construction process can thus go from fine-scale structures, assembled at higher and higher levels into larger structures.

q. Alternatively, electromagnetic construction thus offers the potential to form various other shapes, including long struts and curved structural members. Figure 3-8 shows a structure forming from chains in an electromagnetic field, compared to walls forming in an acoustic resonator in microgravity flight test. The design issue now is to construct the electromagnetic resonator where the axisymmetric electric field required to do this, can be achieved.

3.21 Conclusions

The main findings of this work are listed below:

- Proof-of-concept experiments have been achieved using acoustic force fields, showing the formation of walls of complex shape, single-particle thick.
- A unified prediction capability has been developed for acoustic and electromagnetic force fields.
- An acoustics-electromagnetic analogy has been used to extrapolate electromagnetic field behavior to very low frequencies and predict the energy requirements for building large structures using electromagnetic force fields.

- Validation experiments in acoustics optics and microwave regimes proves the scaling relationships for forces on single particles in both the acoustic and electromagnetic regimes.
- Particle-field interaction and particle-particle interaction are predicted using a dipole model of particle response.
- Along acoustic nodal surfaces, particles repel each other normal to the surface but attract along the surface, forming single-particle thick, stable walls.
- In transverse electromagnetic modes, particles attract normal to the nodal surface, and repel along the surface, thus forming particle chains of different shapes.

3.22 References

[18] Meyer, *Physical and applied acoustics*. 1972, New York: Academic. 123-124.

[19] Torr, *The Acoustic Radiation Force*. American Journal of Physics, 1984. **52**(5): p. 402-408.

[20] Rayleigh, "On the momentum and pressure of gaseous vibrations and on the connection with the virial theorem," Philosophical Magazine, 10, series 6, 364-374, 1905.

[21] Wanis, S., Sercovich, A., Komerath, N., "Acoustic Shaping in Microgravity: Higher Order Shapes," AIAA 99-0954, Aerospace Sciences Meeting and Exhibit, Reno, NV, January 1999

[22] Wang, T., and Lee, C., *Radiation Pressure and Acoustic Levitation*. Nonlinear Acoustics, ed. H.a. Blackstock. 1998: Academic Press. Chapter 6.

[23] Nyborg, W., *Radiation Pressure on a Small Rigid Sphere*. J. Acoust. Soc. Am., 1967. **42**(5): p. 947-952.

[24] Kundt, A., Lehmann, O. (1874). "Longitudinal vibrations and acoustic figures in cylindrical columns of liquids." Annalen der Physik und Chemie (Poggendorff's Annalen) **53**: 1.

[25] Kundt, A., Lehmann, O., *Longitudinal vibrations and acoustic figures in cylindrical columns of liquids*. Annalen der Physik und Chemie (Poggendorff's Annalen), 1874. **53**: p. 1.

[26] Altberg, W., Ann. Phys. (Leipzig), 1903. **2**: p. 405.

[27] King, L.V., *On the acoustic radiation pressure on spheres*. Proc. Roy. Soc., 1934. **A147**: p. 861.

[28] Wanis, S.S., *Tailored Force Fields for Flexible Fabrication*, Ph.D. Dissertation *Aerospace Engineering*. 2006, Georgia Institute of Technology: Atlanta, GA.

[29] Wang, T., and Lee, C. (1998). Radiation Pressure and Acoustic Levitation, Academic Press.

[30] Abramowitz, M., and Stegun, I. (1965). Handbook of Mathematical Functions. New York, Dover.

[31] Ashkin, A., *Acceleration and Trapping of Particles by Radiation Pressure*. Phys. Rev. Lett., 1970. **24**(4): p. 156.

[32] Chu, S., Phys. Rev. Lett., 1986. **57**: p. 314.

[33] Ashkin, A., Dziedzic, J., Yamane, Optical Trapping and Manipulating of Single Cells using Laser Beams. Nature, 1987. **330**: p. 769.

[34] Svoboda, K., Block, S., *Biological applications of optical forces*. Rev. Biophys. Biomol. Struct, 1994. **23**: p. 247-285.

[35] Constable, A., Kim, J., Mervis, J., Zarinetchi, F., Prentiss, M., *Demonstration of Fiber-Optical Light-Force Trap*. Optical Letters, 1993. **18**(21): p. 1867.

[36] McGloin, D. (2004) *Fiber Optical Trapping*. http://www.st-andrews.ac.uk/%7Eatomtrap/Research/Beams/fibre/fibre.htm Viewed Sep. 15, 2006.

[37] Zemanek, P., Jonas, A., Sramek, L., Liska, M., Optics Communications, 1998. **151**(Elsevier Science): p. 273-285.

[38] Harada, Y.a.A., T., *Radiation forces on a dielectric sphere in the Rayleigh scattering regime*. Optics Communications, 1996. **124**: p. 529-541.

[39] Griffiths, D., *Introduction to electrodynamics*. 2nd ed, Z.d.S.a.C. Ferrari. 1989, New Jersey: Prentice-Hall, Inc. 532.

[40] Williams, G.a.T., D., *Phenomenological and molecular theories of dielectric and electrical relaxation of materials*. Application Note Dielectrics 3, 1998: p. 1-28.

[41] Hunter, R., *Foundations of colloid science*. second ed. 2001, New York: Oxford University Press Inc.

[42] Debye, P., Ann. Phys., 1909. **30**(4): p. 57.

[43] Mie, G., Ann. Phys. (Leipzig), 1908. **25**: p. 377.

[44] Metaxas, A.C., *Foundations of Electroheat: A Unified Approach*, ed. U. University of Cambridge. 1996, Cambridge: John Wiley.

[45] Wanis, S., Komerath, N. Use of Radiation Pressure for Space Based Construction. in ASCE Earth & Space. 2004. Houston, TX.

[46] Barmatz, P., personal communication, 2005.

[47] NOAA. *A Primer on Space Weather.* 2006 [cited 2006 April 4, 2006]; Available from: http://www.sec.noaa.gov/primer/primer.html.

[48] Wilson, J.W., Miller, J., Konradi, A., Cucinotta, F.A., "Shielding Strategies for Human Space Exploration", NASA CP 3360, December 1997.

[49] Saiki, T., Uchida, S., Motokoshi, S., Imasaki, K., Nakatsuka, M., Nagayama, M., Saito, Y., Niino, M., Mori, M., "Development of Solar-Pumped Lasers for Space Solar Power Station". IAC-05-C3.4-D2.8.09, IAC2005, Fukuoka, Japan, October 2005.

[50] Rangedera, T., Vanmali, R., Shah, N., Zaidi, W., Komerath, N., "A Solar-Powered Near Earth Object Resource Extractor". Proceedings of the Space Systems Design Conference, Georgia Institute of Technology, Atlanta, GA, Nov. 2005

[51] Komerath, N.M., Satyshur, P., Rangedera, T., Wanis, S.S., "System Design of Large Space Structures Using Tailored Force Fields", AIAA Paper 2006-7323, SPACE2006, San Jose, CA, Sep. 2006.

[52] Wanis, S., Matos, C., Komerath, N., "Acoustic Shaping: Application to Space Based Construction," AIAA 00-1020, January 2000.

[53] Wanis, S., Akovenko, J., Cofer, T., Ames, T., Komerath, N., "Acoustic Shaping in Microgravity," AIAA98-1065, 1998.

[54] Wanis, S., Sercovich, A., Komerath, N., "Acoustic Shaping in Microgravity: Higher Order Shapes," AIAA 99-0954, Aerospace Sciences Meeting and Exhibit, Reno, NV, January 1999

[55] Recent experiments by Wanis using force on a pendulum in an acoustic resonator in ground tests. In Wanis, S.S., "Tailored Force Fields for Flexible Fabrication". PhD Thesis, Georgia Institute of Technology, School of Aerospace Engineeering, May 2006.

[56] King, L.V., "On the Acoustic Radiation Pressure on Spheres," in Proc. Roy. Soc., A147, 1934, pp.861.

[57] Zemanek, P., Jonas, A., Sramek, L., Liska, M., Optics Communications **151**, 273-285 (1998).

[58] Komerath, N., Wanis, S., Czechowski, J., "Tailored Force Fields for Space-Based Construction," Proc. STAIF 2003 AIP CP 654, New Mexico, 2003, pp. 1204-10.

[59] Wanis, S.S., "Tailored Force Fields for Flexible Fabrication". PhD Thesis, Georgia Institute of Technology, School of Aerospace Engineering, May 2006.

[60] Wilson, J.W., Miller, J., Konradi, A., Cucinotta, F.A., "Shielding Strategies for Human Space Exploration", NASA CP 3360, December 1997.

[61] Watkins, J.L., Kackson, H., Barmatz, M., "Measurement of Microwave Induced Forces," in Microwave Processing of Materials III, Materials Res. Soc. Symposium Proceedings, 269, edited by Beatty, W., Sutton, M., Iskander, 1992, pp. 151-156.

[62] Wanis, S., Komerath, N., "Validation of Tailored Force Fields Concept for Use in Space-Based Construction," STAIF-05-081, in the proceedings of the STAIF conference, edited by El-Genk, AIP Conference Proceedings, Albuquerque, NM, Feb. 2006.

4 A Solar-Powered Near Earth Object Resource Extractor

4.1 Introduction

The topic of this chapter is the conceptual design of a solar-powered robotic craft to land on, attach to, and extract materials from, a typical NEO. A solar-powered trajectory to a candidate NEO is used to estimate requirements. A reconfigurable solar sail / collector is the primary propulsion and power source for the craft. Following a journey of nearly 5 years, the craft will use a unique pulsed plasmajet torque-hammer concept to attach to the NEO. The basic cutting tool element is a solar-powered Neodymium fiber laser beam sheathed in a plasma jet, expanded through a truncated aerospike nozzle. Two telescoping, rotating arms carrying a total of 60 such nozzles at the ends of "fingers" enable the craft to dig and "float" out NEO material at a rate adequate to build a 50m diameter, 50m-long, 2m thick, walled cylinder within 19 days. The system is also amenable to applications requiring excavation of a large mass of near-surface material for resource processing. The present design appears to close with a total payload to LEO of 37,500 kg, with a total mass of 30,000 kg including the sail/collector at earth escape. The primary consumables on the system are the plasma gas for cutting and maneuvering, and electrodes of the plasma cutters.

Near Earth Objects (NEOs) offer convenient low-gravity sources of the resources needed to extend a permanent human presence beyond earth, and build a Space-based economy. In previous work[63], we have considered the concept of automatically forming closed wall shapes such as cylinders in Space from solid material of random shape and multidisperse size distribution, using “Tailored Force Fields”. This concept opens the way to building stations with walls massive enough to provide long-term radiation shielding, and strong enough to operate as 1-G artificial gravity modules. In Vanmali et al[64], we laid out the requirements for such a mission to an NEO imagined to be at earth-sun L-4. Here we consider the conceptual design of a robotic machine to do surface excavation on a typical NEO.

Previous work on extraterrestrial resource exploitation has considered harpoons[65] to anchor a drilling craft onto the surface of a NEO in order to drill out material for mining. A nuclear-powered bucket-wheel excavator has been proposed[66] by the Colorado School of Mines, to roll along the lunar surface and scoop up material with a bucket wheel. This machine uses its own weight (on the lunar surface) to apply downward pressure to dig into the ground with the teeth of each bucket. Such a device is suitable for loose sandy material found on planetary surfaces, filling the role of a lifting machine rather than a cutter. The NASA Deep Impact mission demonstrated automatic adjustment of its navigation at high speed to intercept a comet. This demonstrates a solution to part of the problem of robotic NEO rendezvous.

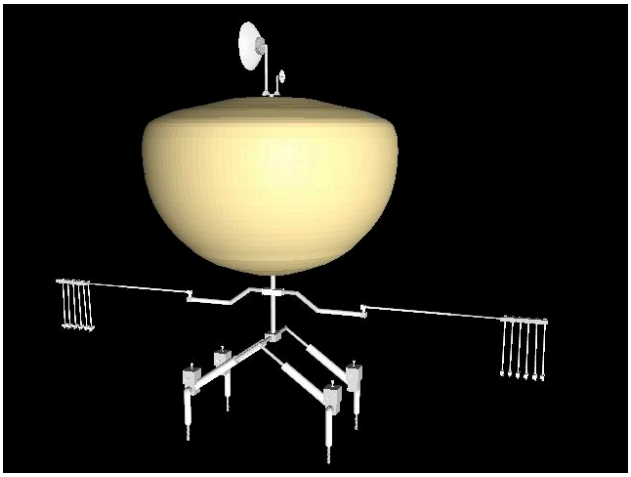

Figure 4-1:Conceptual Drawing of the Rockbreaker robotic NEO resource extractor craft. From Ref. 2

Our interest is in developing a solar-powered solution that can then be used repeatedly away from earth for long-term resource exploitation. The craft thus considered has to be autonomous and versatile. The Rock Breaker described in Ref. 2 (see Figure 4-1) is a multipurpose robotic craft designed primarily to cut rocky material to construct habitats. The craft is to independently rendezvous with a NEO and attach itself. The craft would use plasma jets and laser cutters in order to cut out 20 cm cubic blocks and make them float into a helical cloud away from the NEO. The TFF craft would then form a resonator around the cloud of construction blocks in order to begin the shaping process. The design shares many features with a craft that will be

required for any extra-terrestrial resource exploitation project that hopes to use low-gravity NEOs. In previous work, we conceptualized a trip to Earth-Sun L-4. In this paper, we specialize the mission to a 'typical' choice of Near Earth Object.

4.2 NEO Population

NEOs are classified by absolute magnitude, semi-major axis, aphelion/perihelion distance, and composition. The NEO population is composed of asteroids, active comets, and extinct comets. Subcategories of the NEO population are Atens, Apollos, and Amors. Their size range from dust-sized fragments to objects tens of kilometers in diameter[67]. The lower limit of detectability is generally on the order of a few hundred meters diameter. Roughly 1000 NEOs have been found, of which around 100 are accessible with mission delta-v comparable to that for lunar missions, though the mission time may be on the order of years[68]. Christou[68] provides guidance in selecting NEO mission destinations. Objects in orbits similar to that of Earth are the easiest and fastest to reach. An orbit eccentricity range of $0.3<e<1.2$, and an inclination limit of 5°, along with limits on object size, still leaves at least 27 possible NEOs. One possibility is 1996 FG3.

4.3 Requirements Definition for the Mission

The requirements for the Rockbreaker are given in Table 4-1, modified from Ref. (54).

4.3.1 Solar Sail

Given that most early NEO missions will be near the orbit of Earth, and these missions are not time-critical unlike human spaceflight, solar sail propulsion is an attractive choice. Since the solar sail is a low thrust spacecraft, it is difficult to find the best possible trajectories because it involves an in depth knowledge of numerical optimal control methods. Our approach at this conceptual design stage is to use trajectories calculated by other researchers, and scale the sail area needed using the payload-to-sail-area ratio.

Table 4-1. Mission requirements of the Rock Breaker

Requirement	Assumptions / choices
Single unit launch from Earth.	Avoid on-orbit assembly costs.
Travel to L-4 using solar propulsion	Minimizes launch mass and takes advantage of the 1 A.U. destination.
Rendezvous with a low-gravity NEO	NEO size is only a few kilometers.
Attach itself to the NEO in order stay anchored while cutting	Removable attachment means suitable for many sorts of surfaces.
Cut out a large amount of material in the form of discrete blocks, within a short time and loosen the blocks enough to float apart at controlled speeds.	Discrete blocks is a conservative choice; blasting is presumed to be unacceptable because of poor control on ejection velocity
Detach itself and move to another location on the same NEO, or leaving the NEO.	Craft used for repeated quarrying/ assembly/ resource extraction, with possible refill of cutting / maneuvering gas.
Use manipulator arms and power delivery systems to inspect cut pieces, and/or subject them to heating and gas jets for preliminary sampling and separation.	Plasma or laser heating, or microwave heating. Detectors and probes at arm tips.
Hold and guide large sintered pieces into position. Weld/ sinter them in place	Entire craft to maneuver, and robotic arm for precision.
Move to another NEO to quarry resources for future consumption	Redeploy solar sail.

Dachwald and Seboldt[69] used artificial neural networks (ANNs) along with evolutionary neurocontroller algorithms (EAs) to optimize for solar sail craft trajectories. We use their calculations of a solar sail mission to 1996FG3 "InTrance". A total sail craft mass of 148 kg (75 kg payload and 73 kg sail assembly) would have a 2500 sq.m sail area. Characteristic acceleration was on the order of

$0.14mm/s^2$. The transfer time was 4.15 years starting from earth escape. The characteristic acceleration is due to the solar radiation pressure (SRP) acceleration acting on the solar sail that is oriented perpendicular to the sun-line at 1 AU. Technology advances can be used to increase sail area for the same mass, thereby increasing the characteristic acceleration and reducing the transfer time significantly[5]. Alternatively, the total craft mass can be reduced. The Dachwald/ Seboldt design envisages total sail craft loading of $59.2\ g/m^2$. Scaling the sail area needed for the same trajectory, we see that the sail area needed for our mission would be 833,000 sq.m, and the total craft mass, for a 25,000 kg Rockbreaker craft, would be 49,333 kg. Recent experiments[70] have demonstrated a nested sail deployment concept, which promises area density of $0.01\ kg/\ m^2$. With this technology, the sail mass can be reduced, and the sail area required is less than 510,000 sq.m. The total mass at Earth escape would be just over 30,000 kg, consisting of a 25,000 kg Rockbreaker craft, and a 5080 kg solar sail assembly.

4.4 Power Generation and Transmission

As the craft reaches its destination, its systems are "woken up". The 0.5 sq. km solar sail is formed into a solar collector, focusing sunlight directly to the power supplies of laser system, and on high-intensity solar cells to power other systems. In Ref. 2 we had proposed not locating power conversion systems on the Rockbreaker, since they were believed to be quite massive. Instead, they were to be located on the "Tailored Force Field" craft used to form the rubble cut up by the Rockbreaker into structures of desired shape. This posed challenges in beaming microwave power from the TFF craft to the Rockbreaker.

Recently, efficiencies of up to 38% have been achieved in the laboratory[71] in converting broadband sunlight directly to 1064-nm laser radiation using a Cr_2-doped Nd-fiber laser. This breakthrough is well suited to our application, since the primary tool used by the Rockbreaker is a Nd-fiber laser cutting tool. We can replace the Nd fiber laser with the Chromium-doped Nd fiber laser, and eliminate the need for conversion equipment to go from solar power to DC and then microwave. This is a huge mass saving, and it removes the argument in our previous work for tying the Rockbreaker to beamed microwave power from converters on the Force Field Tailoring craft.

4.4.1 Cutting System

The system conceived to cut material from the surface of the NEO is adapted from what Ref. 2 proposed for the mission to cut building blocks for a habitat module. It consists of six lasers each of 25KW, conveying pulsed beams to 60 nozzles arranged at the "fingertips", five to each arm, of 12 cutting arms, each laser beam sheathed in an annular plasma jet.

4.4.2 Laser Cutter

We propose evolved versions of the above laser to perform most of the cutting functions of the Rockbreaker. As described in Ref. 2, laser cutting tools have very low tool attrition[72,73], enabling maintenance-free operation for long periods with a variety of materials. The laser offers the highest power density available in the industry[74] and are two orders of magnitude faster than rotary drills for rock drilling[75]. The Nd fiber laser offers 10 w/kg and long operating lifetime[76,77] exceeding 100,000 hours[78], compared to 10,000 and 25,000 hours respectively for Nd-YAG and CO_2 lasers. A single fiber strand of a few microns can already generate and deliver over 1kW; this is expected to rise considerably[79,80,81,82].

A typical 700W fiber laser generates a beam intensity of more than $50MW/cm^2$. A beam power density of less than $1kW/cm^2$ sufficed[83] to cause thermal spalling of sandstone and shale, both of which have similar densities to silicon dioxide. The major uncertainty about NEOs is their composition. Given this uncertainty, the latent heat of melting of silicon dioxide was used in our calculations, assuming that 25% of the energy required for melting sufficed to crack the material. Fusion cutting, where laser energy melts and cracks the material, and a gas jet blows out the debris, requires only 10% of the power and 3% of the time for vaporization cutting[84].

4.4.3 Plasma Cutting Mechanism

A plasma jet sheath around the laser beam was proposed in Ref. 54, to blow away the material being heated and fractured by the laser, and expose fresh material to the laser beam[85]. Non-metallic NEO

materials are amenable to a non-transferred plasma jet, where the torch nozzle becomes the anode. The pressures, standoff distance and nozzle expansion ratio are parameters used in optimizing the cutting trench width and the stagnation pressure exerted on the cut blocks (see Figure 2) to move them in desired directions (including the original objective of floating them away from the NEO for the construction application).

The electrodes are consumables that require periodic replacement; currently at less than 1000 hours. Generating a thin jet sheet in vacuum presents substantial difficulties, for which the aerospike nozzle provides some solutions. The storage volume and mass on the craft limit the amount of gas that can be carried for the plasmajet, so that minimizing the mass flow rate is critical. Electrode attrition and gas mass severely restrict use of the plasmajet.

4.4.4 Hybrid Aerospike Cutting System (HACS)

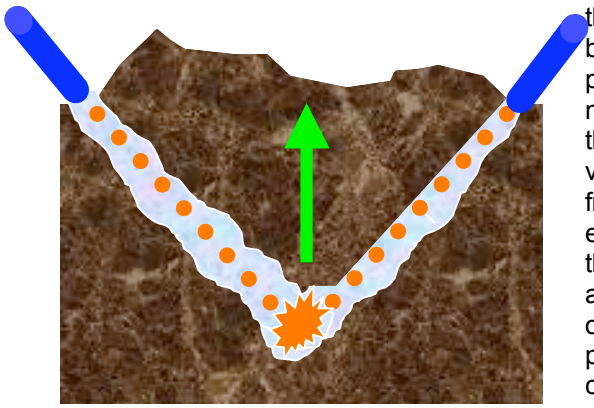

Figure 4-2:HACS operation, showing force exerted on the blocks by the plasmajet

A hybrid laser and plasma cutting system is proposed for the Rock-Breaker design. The main cutting tool that breaks up the surface material is the laser, while the plasma jet finishes the process by removing waste material from the trench and pushing the block towards the TFF craft. The HACS is lowered from the craft on a vertical pillar. HACS two main booms and can extend from the craft using its telescoping feature. At the end of each boom are 6 arms to lower 10 cutting nozzles each to the ground. Contained in each arm is a laser. The two arms rotate around the pillar in the vertical axis. The outcome is a spiral-cutting pattern. The rotor design, spiral pattern, and telescoping arms maximize the surface area covered by the HACS, and thus the amount of material that can be cut when the craft is anchored in one location. Ref. 2 described an optimized cutting sequence to generate the most cut blocks in minimum time. This is matched to the rotating/telescoping arm and multiple-fingers design.

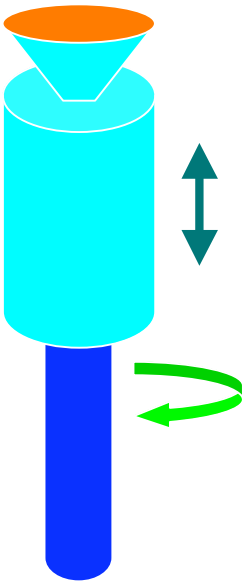

Figure 4-3: Impact Driver

4.4.5 Truncated Linear Aerospike Cutting Nozzle

A linear truncated aerospike nozzle[86] design is employed, similar in concept to that in the X-33 vehicle. The linear design stacks several modules to produce an effective “knife edge”. The laser beam is directed through the truncated base into the recirculation zone downstream, which adjusts itself to the pressure of the jet, forming a virtual spike. The laser beam is thus sheathed in a high-speed plasma jet, while the flow immediately in contact with the laser delivery lens remains at a low speed. The jet sheath and the recirculating base flow region protect the delivery lens from abrasion.

4.4.6 Integrated Rendezvous-Anchoring Maneuver-System (IRAMS)

NEO rendezvous is complicated by NEO spin/tumble, which will demand considerable maneuvering delta-v. Reactions from any cutting operation must be absorbed by anchoring the vehicle on the surface of the NEO. We use a concept derived from the Impact Screwdriver that converts an axial, impulsive load to torque, matching the dynamics of the system to a pulsed solid-grained plasma thruster. Each leg of the vehicle is provided with an IRAMS pulsed plasma thruster which can be oriented in any direction for maneuvering. At the terminal stage of rendezvous, each leg approaches the NEO surface with a large-pitch, deep-thread screwdriver (or drill-bit) facing the surface. At impact, the inertia of the system translates into the first torque.

Following landing, the plasma thruster operates in short bursts, with the reaction driving the solid fuel grain into the torque hammer groove, causing high torque on the spring-loaded threaded tool (Figure 3). Ten to twenty centimeters of travel into the surface, depending on its hardness and brittleness, will suffice to anchor the craft in place. Being a mass-spring system, the IRAMS can be optimized. We started by setting up a dynamical model of the IRAMS and then using this model to obtain the natural frequency combination that would produce the highest amplitude.

Pulsed, solid-grained plasma thrusters[87] offer precise pulsed operation, cold start, intermittent duty cycles and reliable, storable solid grain. They are thus the best choice for long-term operation. Again, the solid grain is a consumable, but it is not expected to be a limiter of the craft's lifetime. As shown in Ref. 2 the time between pulses depends on the natural frequency of the system, which should be matched with the thrust pulse rate to minimize power loss from thrust to torque output.

4.5 Auxiliary Systems

4.5.1 Active beam dynamics

The pulsed thrust of the plasmajets from the 60 independent nozzles will be phase-controlled to cancel out all but the lowest-order modes of bending of the Rockbreaker's arms during the cutting operation. This will also be used to control the arms during use as manipulators.

4.5.2 Sensor Systems

Sensor systems special to this craft, beyond those required for a standard spacecraft, include ground penetrating radar (GPR), which has been used on Earth to map geophysical properties[88] under the surface. Its role on the Rock-Breaker is to scout out favourable areas on the surface of the NEO before anchoring onto a location. The system to be used has an antenna frequency range of 0.5 - 1 GHz for medium to shallow penetration with a high-resolution radar survey. Optical sensors will be needed to control the temperature of the materials being heated by the Rockbreaker, as well as to see obstacles and samples.

4.5.3 Propellant Fuel Tank

The plasma jets feed off an argon[89] propellant tank. The tank structure mass is calculated at 5% of the total propellant mass. The plasma jet in its current application has an estimated power range of 1-10kW and current not exceeding 200A[90]. For these limitations, the mass flow rate range is 0.03-1.2g/s[91,92].

4.5.4 Robotic Manipulator Operations

The robotic arms have enough degrees of freedom to be ideal as manipulator arms. The four deployable legs with the IRAMS enables precise maneuvering of the craft.

4.6 Mass Estimation

In Table 4-2, the mass of the various components is estimated. The operating duration and mass excavation capability were calculated in Ref. 2 using the requirements for the Tailored Force Fields project, where each Rockbreaker was sized to cut up enough blocks of SiO2-class material to form a closed cylinder 50m diameter and 50 m long, with a 2m thick wall. The mass to be excavated was twice this amount, since 50% wastage was assumed. The number of nozzles, and the power delivery rate, were calculated to generate this amount of material with 19 earth-hours of continuous operation at Earth-sun L-4. This time was considered appropriate because, with a 1cm/sec initial drift velocity after overcoming the gravity of the NEO, the mass generated could be collected in an approximately toroidal cloud a few kilometres away from the NEO in that time, to perform the shaping and sintering. These parameters are considered to be adequate as a starting design for a more general-purpose excavator/ resource extractor craft.

Table 4.2: Component Mass Breakdown

Component	Mass (kg)
IRAMS, Thrusters (propellant included)	1000
HACS	2000
Power conversion system (other than lasers) incl. high-intensity solar cells.	1200
Plasma/Laser Cutting System	15000
Propellant Tank (argon)	200
Argon gas	4000
Communications antennae	50
Sensor suite	300
Manipulator arms	500
Protective Covering	200
Thruster Propellant (for maneuvering)	500
Total payload	24950
Solar Sail	5080
Booster + auxiliary propellant	7500
Total propulsion package	12580

The majority of the mass is the laser/plasma cutting system, which is based on lasers currently available, assuming 10W/kg. The HACS is built with a network of hollow aluminum alloy rods strong enough to withstand the force of the plasma jets at the ends with active compensation as indicated above. Its weight is determined by its density (2700kg/m^3) and the length of each section. The present Space Shuttle Manipulator Arm (Canadarm) has a mass[93] of 410 kg, and is sized to move the entire STS Orbiter (120,000 kg) at acceptable rates for rendezvous with the ISS, so the HACS estimate is reasonable and conservative. Solar sail construction is by the method mentioned at the beginning of the paper, and targets an aereal density of 10g per square meter. The mass of argon gas was found using the mass flow rate of 0.03g/s feeding to 60 nozzles over a period of 460 hours. The propellant mass required for drilling, anchoring and re-anchoring is included in the IRAMS component; the amount required for moving the Rock-Breaker from the rendezvous point to NEO surface and other maneuvering tasks is in the thruster propellant mass.

The mass estimate in Table 2 is broken into two packages. The first is the basic Rock-Breaker craft, which is the payload to be propelled by the solar sail. The second is the solar sail package itself, along with a 7500 kg boost package to take the craft and sail from LEO to a transfer orbit where the sail can be deployed. The boost package mass is ample for an electric thruster system to send the craft into an earth escape trajectory. It is seen that one of the new NASA launchers can lift the entire package to LEO or even into a transfer orbit, thereby making on-orbit rendezvous unnecessary.

4.7 Conclusions

This chapter describes the approach to design a new kind of spacecraft for extraterrestrial construction and resource exploitation applications. Solar propulsion, beamed microwave power, and fiber laser and plasma jet cutting tools, and an Integrated Rendezvous, Anchoring and Maneuvering System are explored, and their issues considered. Conclusions are:

- Solar sail primary propulsion appears to be well suited to the NEO application.
- With direct solar-pumped Nd-fiber lasers, the solar sail of a single craft would suffice to act as a solar collector and provide continuous power for operations.
- With the new generation of launch vehicles announced under the Moon-Mars initiative, a Rockbreaker and the propulsion package for boost to an earth-escape trajectory, can be launched assembled in a single launcher to low earth orbit.

4.8 References

[63] Wanis, S., Komerath, N., "Advances In Force Field Tailoring For Construction In Space". IAC05-D1.1.02, 56th International Astronautical Congress, Fukuoka, Japan, October 2005.

[64] Vanmali, R., Li, B., Tomlinson,B., Zaidi, W.,, Wanis, S., Komerath, N., "Conceptual Design of a Multipurpose Robotic Craft for Space Based Construction". AIAA Paper 2005-6733, SPACE 2005 Conference, Long Beach, CA, Aug. 2005

[65] NASA FACT SHEET: Asteroids, Comets, and NASA Research. http://meteorite.org/facts.htm

[66] Muff, T., Johnson, L., King, R., Duke, M.B., "A Prototype Bucket Wheel Excavator for the Moon, Mars and Phobos". Proceedings of STAIF 2004, Institute for Space and Nuclear Power Studies, Feb. 2004, p. 214.

57. Bottke, W. F., Morbidelli, A., Jedicke. R., Petit, J., Levison, H.F., Michel, P., and Metcalfe, T.S., 2002. Debiased Orbital and Absolute Magnitude Distribution of the Near-Earth Objects. Icarus 156, 399-433.

[68] Christou, A.A., 2003. The Statistics of flight opportunities to accessible Near-Earth Asteroids. *Planetary and Space Science* 51, 221-231.

[69] Dachwald, B., Seboldt, W., "Multiple Near-Earth Asteroid Rendezvous and Sample Return Using First Generation Solar Sailcraft". Acta Astronautica, Pergamon Press, August 2004. http://www.sciencedirect.com

[70] Wilcox, B.H., "Nesting-Hoop Solar Sail". NASA Tech Briefs, Vol. 24, No.9, September 2000.

[71] Saiki, T., Motokoshi, S., "Development of Solar-Pumped Lasers for Space Solar Power". IAC-05-C3.4-D2.8.09, 56th International Astronautical Congress, Fukuoka, Japan, October 2005.

[72] Steen, W.M., *Laser Material Processing*, 2nd ed., Springer, London, 1998, pp. 104.

[73] Gahan B., Batarseh S., Siegfried R., "Improving Gas Well Drilling and Completion with High Energy Lasers," National Energy Technology Laboratory Strategic Center for Natural Gas & Oil, Argonne National Lab., DE-FC26-00NT40917, Des Plaines, Illinois.

[74] Steen, W.M., *Laser Material Processing*, 2nd ed., Springer, London, 1998, pp. 50.

[75] Gahan, B., Shiner B., "New High-Power Fiber Laser Enables Cutting-Edge Research," *GasTIPS*, 10,1, 2004, pp. 29-31.

[76] Trumpf Inc. North America, Brochure. "TRUMPF TLF Lasers".

[77] IPG Photonics. CW Industrial Fiber Lasers: 1kW to 20kW Output Optical Power.

http://www.ipgphotonics.com/html/115_cw_fiber_lasers.cfm Viewed Aug. 6, 2005

[78] Shiner, B., "High-power fiber lasers impact material processing," *Industrial Laser Solutions*, 2003.

[79] Jeong Y., Sahu J.K., Payne D.N., Nilsson J., "Ytterbium-doped large-core fiber laser with 1kW of continuous-wave output power," *Electronics Letters*, Vol. 40, No. 8, 2004, pp. 470-472.

[80] Liem A., Limpert J, Zellmer H., Tunnermann A, Reichel V., Mörl K., Jetschke S, Unger S., Müller H.R., Kirchof J., Sandrock T., Harschak A., "1.3kW Yb-doped fiber laser with excellent beam quality," *Proceedings of Conference on Lasers and Electro-Optics 2004*, San Francisco, USA, May 2004.

[81] Jeong Y., Sahu J.K., Payne D.N., Nilsson J. "Ytterbium-doped large-core fiber laser with 1.3kW continuous-wave output power," *Optics Express*, Vol. 12, No. 25, 2004, pp. 6088-6092.

[82] Payne D.N., Jeong Y., Nilsson J., Sahu J.K., Soh D.B.S., Alegria C., Durpriez P., Codemard C.A., Philippov V.N, Hernandez V., "Kilowatt-class single-frequency fiber sources", Proc*eedings of SPIE – Fiber Lasers II: technology, systems, and applications: 24-27 January 2005*, San Jose, California, USA., International Society for Optical Engineering, Vol. 5709, Bellingham, 2005.

[83] Gahan, B., "Laser Drilling: Understanding Laser/Rock Interaction Fundamentals," *GasTIPS*, 8, 2, 2002, pp. 4-8.

[84] Steen, W.M., *Laser Material Processing*, 2nd ed., Springer, London, 1998, pp. 110.

[85] Ramasamy R., Selvarajan V., "Current-voltage characteristics of a non-transferred plasma spray torch," *The European Physical Journal. D, Atomic, molecular, and optical physics*, 8, 1, 2000, pp. 125-129.

[86] "Rocket Nozzle Shapes" from Huzel & Huang, 1967.

http://www.aerospaceweb.org/design/aerospike/shapes.shtml

[87] Pulsed Plama Microthrusters. http://www.mae.cornell.edu/ campbell/mppt/mppt.htm

[88] Olhoeft, G.R., "Applications and frustrations in using ground penetrating radar," *Aerospace and Electronics Systems Magazine, IEEE*, Vol. 17, No. 2, 2002, pp. 12-20.

[89] Venkatramani, N., "Industrial plasma torches and applications," *Current Science*, 83, 3, 2002, pp. 254-

[90] Hypertherm Inc. Manual Product Line http://www.hypertherm.com/manual/index.htm

[91] Bauchire J.M., Gonzalez J.J., Gleizes A., "Modeling of a DC Plasma Torch in Laminar and Turbulent Flow," *Plasma Chemistry and Plasma Processing*, 17, 4, 1997, pp. 409-432.

[92] Kelly, H., Mancinelli B., Prevosto L., Minotti F.O., Marquez A., "Experimental Characterization of a Low-Current Cutting Torch," *Brazilian Journal of Physics*, 34., 4B, 2004, pp. 1518-1522.

[93] Garneau, M., "CANADARM". STS97, Canadian Space Agency Website. http://www.space.gc.ca/asc/eng/missions/sts-097/kid_canadarm.asp Viewed August 6, 2005.

5 Publications & Outreach

5.1 Degrees Awarded:

5.1.1 PhD Theses

Sameh S. Wanis, ""Tailored Force Fields for Flexible Fabrication" PhD Thesis, Georgia Institute of Technology, School of Aerospace Engineering, May 2006.

5.1.2 M.S. Special Problems Reports

Patrick Satyshur, "Modeling and simulation of Tailored Force Fields" May 2006

Sameer Hameer, "Beamed Microwaves for Space Power", August 2005

Cedric Justin, "Particle Dynamics in an Electromagnetic Field", December 2006.

5.2 Awards Won

James Nally, GIT Presidents's Undergraduate Research Fellowship 2005
Nicholas Boechler, NIAC Student Fellowship, 2005-2006
Sam Wanis, Sam Nunn Pre-Doctoral Security Fellowship, 2005
Thilini Rangedera, GIT Presidents's Undergraduate Research Fellowship 2005

5.3 Chapters in Books/ Proceedings

Komerath, N.M., "Space Stations". in "USA in Space" Encyclodopaedia", 3rd Edition, Salem Press, February 2006

5.4 Peer-Reviewed Publications

Wanis, S.S., Komerath, N.M., "Use of Radiation Pressure for Space-Based Construction". Proceedings of the ASCE "Earth and Space 2004" Conference, Albuquerque, NM, March 2004.
ASCE American Society of Civil Engineers, Virginia, 2004.

Komerath, N.M., Wanis, S.S., Czechowski, J., "Tailored Force Fields for Space-Based Construction". Proceedings of the STAIF Conference, Albuquerque, NM, February 2003.

Komerath, N.M., Wanis, S.S., "Radio Waves for Space-based Construction". Proceedings of the STAIF 2004 Conference, Albuquerque, NM, February 2004.

Ravi Vanmali, Brandon Tomlinson, Bryan Li, Sam Wanis, Narayanan Komerath, "Engineering a Space Based Construction Robot". Paper 05WAC-44, Proceedings of the SAE World Aerospace Congress, October 2005

Wanis, S., Komerath, N.M., "Validation of TFF Concept for Use in Space Based Construction". STAIF 06-081. In El Genk, Editor, Proceedings of the Space Technology and Applications International Forum, American Institute of Physics Conference Proceedings Volume 813, Albuquerque, NM, Feb. 2006, ISBN: 0-7354-0305-8

Boechler, N., Hameer, S., Wanis, S., Komerath, N.M., "An Evolutionary Model for Space Solar Power". In El Genk,

Editor, STAIF 06-082, Proceedings of the Space Technology and Applications International Forum, American Institute of Physics Conference Proceedings Volume 813, Albuquerque, NM, Feb. 2006, ISBN: 0-7354-0305-8

Komerath, N.M., Rangedera, T., Nally, J., Space-Based Economy Valuation, Analysis, and Refinement. AIAA Paper 2006-7204, Space 2006, San Jose, CA
Sep.2006 http://www.adl.gatech.edu/archives/adlp06091901.pdf

Komerath, N.M , Satyshur, P., Rangedera, T., Wanis, S.S.,, System Design of Large Space Structures Using Tailored Force Fields, AIAA Paper 2006-7323, Proceedings of the Space Architecture Symposium, San Jose, CA Sep. 2006.
http://www.adl.gatech.edu/archives/adlp06092401.pdf

Komerath, N.M., Boechler, N., "The Space Power Grid". Paper IAC06-D3.4.06, Proceedings of the 56th International Astronautical Congress, Valencia, Spain, October 2006.
http://www.adl.gatech.edu/archives/adlp06100501.pdf

Wanis, S.S., Komerath, N.M., "Force-Field Tailoring: First-Principles Derivation of Wall-Formation Physics". Paper IAC06-D3.2.05, Proceedings of the 56th International Astronautical Congress, Valencia, Spain, October 2006. Abstract hyperlinked:
http://www.adl.gatech.edu/archives/adlp06100301.pdf

Wanis, S.S.. Komerath, N.M., "Particle-Particle Interaction in Electromagnetic Fields for Force-Field Tailoring". Proceedings, American Institute of Physics, STAIF-07, February 2007.

5.5 Conference Papers

B. Tomlinson, B. Li, R. Vanmali, S.Wanis, N. Komerath, "Conceptual design of a Multipurpose Robotic Craft for Space Based Construction". AIAA Paper, Space 2005, Aug-Sep 2005.

Komerath, N.M., "Global Cooperation in an Age of Security Concerns". AIAA 2005-6638,Space 2005, Aug.-Sep 2005

Komerath, N.M., Nally, J., Tang, E. Z. "Policy Model for Space Economy Infrastructure" IAC2005_D3.1.1.08, International Astronautical Congress, Fukuoka, Japan October 2005

Wanis, S.S., Komerath, N.M., "Flexible Space Construction using Tailored Force Fields", IAC2005_D1.1.02, International Astronautical Congress, Fukuoka, Japan October 2005

Nally J.A., Komerath, N.M., "Modeling and Analysis of the Interactions in a Space-Based Economy". Proceedings of the Space Resources Utilization Roundtable, League City, TX, October 2005

Wanis, S., Komerath, N.M., "Tailored Force Fields for Flexible Space-Based Manufacturing". Proceedings of the Space Resources Utilization Roundtable, League City, TX, October 2005

Rangedera, T., Vanmali, R., Shah, N., Zaidi, W., Komerath, N., "A Solar-Powered Near Earth Object Resource Extractor". Proceedings of the Space Systems Design Conference, Georgia Institute of Technology, Atlanta, GA, Nov. 2005

Komerath, N., Boechler, N., Wanis, S., "Space Power Grid- Evolutionary Approach To Space Solar Power". Proceedings of the ASCE Space and Earth 2006 Conference, League City, TX, March 2006

Vanmali, R., Shah, N., Komerath, N., Satyshur, P., "A Robotic Constructor-Excavator for NEO quarrying". Proceedings of the ASCE Space and Earth 2006 Conference, League City, TX, March 2006

Sylvan, R., Komerath, N., Wollert, K., Tang, E.Z., Homnick, M., Palaia, J., "The Emerging Inner Solar System Economy". Proceedings of the ASCE Space and Earth 2006 Conference, League City, TX, March 2006

Wanis, S., Komerath, N., "Designs for Space-Based Construction Using Force Fields", Proceedings of the ASCE Space and Earth 2006 Conference, League City, TX, March 2006
Wanis, S.S., Komerath, N.M., Force-Field Tailoring: First-Principles Derivation of Wall Formation Physics". IACD3.2.05, 57th International Astronautical Federation Congress, Valencia, Spain, October 2006.
Komerath, N.M., Boechler, N., "The Space Power Grid". IAC-C3.4.06, 57th International Astronautical Federation Congress, Valencia, Spain, October 2006.

5.6 OutReach

Komerath, N.M., "Tailored Force Fields for space-based constrtuction". Invited Lecture, Inventors of Georgia Business Meeting, May 2003.

Komerath, N.M., "Tailored Force Fields For Space-Based Construction: Key To A Space-Based Economy" Invited presentation, Government Engineering College, University of Calicut, Thrissur, India, December 2003.

Komerath, N.M., "Building Cities in Space". Invited presentation, TKM Engineering College,University of Kerala, Kollam, India, December 2003.

Komerath, N.M., "Building Cities in Space ". Invited presentation, , Amrita Engineering College,University of Kerala, Amritapuri, India, December 2003.

Komerath, N.M., "Building Cities in the Sky: Problem-Solving Across Disciplines". Invited presentation, Amrita Institute of Technology, Coimbatore, India, December 2003.

Komerath, N.M., "Styrofoam to Space Cities: A Synopsis of the "Tailored Force Fields" Team project". Invited presentation, Southeastern NASA Space Grant Consortium Meeting, Atlanta, GA, February 2004.

Komerath, N.M., Gopalakrishnan, P., Wanis, S.S., "Cities in Space: Articulating the Space Based Economy". Presentation to the Boeing – NASA Aerospace Technology Working Group, Boeing Auditorium, Huntsville, AL March 2004.

Komerath, N.M., Nally, J., Tang, E. Z. "Policy Model for Space Economy Infrastructure" Presented to the Mars Society, Georgia Institute of Technology, January 2006.

5.7 Participation of High School Students

Six NASA SHARP scholars worked with our group, from Summer 2003-summer 2005.

6 Transition Efforts

The focus of the project in the past six months has been on developing the tools and products for transitioning the project into further development.

6.1 Particle Dynamics / Shape Formation Simulator

A time-dependent simulation is now working with nearly 100 particles, forming into shapes in electromagnetic force fields. The field calculations are done for given geometries and wall boundary conditions using the "COMSOL" fine element electromagnetic simulation software. This can be done with a few particles present but stationary inside the resonator in order to develop quantitative measures for interaction between the field and particles.

The time-dependent code uses the pre-determined basic field, along with models for the particle interaction, to capture particle behavior as they come close, and form into structures. These simulations are already working in 3-D for acoustics, where the interaction forces are stronger, but take more time steps in the case of electromagnetics.

This is being refined into a tool that can be used for routine exploration to build up a library of modes and structure shapes for different particle properties.

6.2 2. Large-scale electromagnetic force field demonstration

Discussions are underway to plan testing at the NASA Langley High Intensity Radiation Laboratory. There is mutual interest in an experiment where large particles suspended on strings would be used to explore, quantify and demonstrate mutual interaction and possibly structure formation at a much larger size scale in electromagnetic fields than has been done before.

Summary

This project explored the concept of forming structures in space using solid material, formed into desired shapes by standing wave fields. The idea of tailoring force fields to build structures, has applications over a wide range of sizes. At one extreme is the idea of forming structures on the 100meter scale, using rocks moved into position by a resonant radio-frequency field. If this can be done using material from extraterrestrial sources, it would be possible to build structures massive enough to offer adequate radiation shielding for long-term habitats. This report summarizes the work done during a Phase 2 of the Tailored Force Fields concept. The force predictions are tied to first principles, and to results from several fields. A unified description of acoustic and electromagnetic force fields has been developed and validated through physical and numerical experiments. While the primary force field on individual particles is directly analogous between acoustic and electromagnetic fields, the secondary particle interactions are quite different. A dipole model is used to show that electromagnetic fields can be used to form linear and curvilinear components, while acoustics can fabricate entire walls of specified shape and single-particle thickness. The frequencies used for formation, refinement and fusing of structures are well separated.

Concepts for taking construction machines to Near Earth Objects were studied, as an extreme example of a direct approach to building habitats. In this approach, robotic extractors that would generate the loose NEO material to be formed into thick-walled modules by a solar-powerd resonator. In the vicinity of the NEO. The systems for this approach were reduced to a set of 30,000 kg craft leaving earth orbit. Solar-sailed primary propulsion would takethe craft from earth orbit to NEOs in the near solar system. Solar sails would be reconfigured into collectors to power the devices at the NEO. Strong disadvantages of this approach were that the material extraction (the Rockbreaker operation) had to be synchronized with the force-field tailoring, and the modules would be built at the orbit of the NEO, with further propulsion needed to bring the module to a useful orbit.

An alternative approach considered, was to proceed through a series of small experiments in earth orbit. This approach offered the advantage of telepresence operation. While this offered short-term risk mitigation, it offered no path to building using extraterrestrial material.

A space manufacturing architecture incorporating acoustic and electromagnetic techniques is proposed as the best approach, incorporating strengths of both approaches above. In this architecture, solar-powered resource extractors would generate materials from NEOs, and return the material using solar-sailed craft, to earth orbit. Manufacturing facilities in earth orbit, formed from expended rocket parts, would form this material into useful components that would then be assembled using telepresence. Such an architecture would open the way to building components and assembling large habitats in Earth orbit under telepresence control. Long term space presence requires the construction process to occur in space with the utilization of in-situ resources.

Interest generated by this project had led to the completion of a doctoral dissertation dealing with the understanding of the primary and secondary forces on particles in a resonant field. A rudimentary prediction capability has been developed, ranging over several orders of magnitude in particle size and wavelengths, including acoustic and electromagnetic fields. Under a sub-contract, PSI Corp has studied the design of resonators and power supplies suitable for use in forming large structures in Space.

Table of Contents